NOLTR 63-82

DETERMINATION OF THE ENERGY OF A PULSED LASER BEAM BY TRANSFER OF THE PHOTON MOMENTUM TO A BALLISTIC TORSIONAL PENDULUM

10 SEPTEMBER 1963

NOL

UNITED STATES NAVAL ORDNANCE LABORATORY, WHITE OAK, MARYLAND

NOLTR 63-82

DETERMINATION OF THE ENERGY OF A PULSED LASER BEAM BY TRANSFER OF THE PHOTON MOMENTUM TO A BALLISTIC TORSIONAL PENDULUM

Prepared by:
M. Stimler

ABSTRACT: An instrument has been designed and constructed which is capable of measuring high energies of pulsed laser beams, without seriously interfering with their simultaneous use in an experiment. Transfer of the photon momentum of the beam to angular momentum of a doubly-reflecting ballistic torsional pendulum was the principle by which photon momentum effects were successfully measured. The instrument operates at 10^{-5} mm of Hg with a sensitivity of 2.55 $\pm$ 0.04 cm/joule, and does not require damping of the initial oscillations before making a measurement. In addition to providing the capability of simultaneous energy measurement and use of a laser beam, the measurements made with this instrument appear to be more accurate than with a commercial calorimeter used for comparison.

PUBLISHED OCTOBER 1963

U. S. Naval Ordnance Laboratory
White Oak, Silver Spring, Maryland

NOLTR 63-82 10 September 1963

This report presents the results of an experiment in which the photon momentum of a pulsed laser beam was used to make a fundamental measurement of the beam energy. The work was performed under "New Component Developments", WEAPTASK No. RREN-04-322/212/1/F008-21/02. The report will be of interest to anyone concerned with laser energy measurements.

R. E. ODENING
Captain, USN
Commander

R. E. Grantham

R. E. GRANTHAM
By direction

TABLE OF CONTENTS

TABLE OF CONTENTS (concluded)

LIST OF TABLES

LIST OF FIGURES

LIST OF FIGURES (concluded)

LIST OF SYMBOLS

E = Laser output energy

p = Total photon momentum

m = Associated photon mass

c = Velocity of light in free space.

C = Capacitance in photocell circuit

d = Peak scale deflection

d_o = Peak scale deflection before laser actuation

d_s = Peak scale deflection after laser actuation.

D = Distance of scale from suspension wire

R = Radial distance of suspension wire to center of each reflecting vane.

θ = Peak angular deflection of suspension assembly from rest position.

θ_o = Peak angular deflection of suspension assembly before laser actuation

θ_s = Peak angular deflection of suspension assembly after laser actuation

α = Peak angular deflection of reflected galvanometer-scale indicator from zero position

k = Torque constant of suspension wire

I = Moment of inertia of suspension assembly

T = Period of oscillation of suspension assembly with negligible damping

λ = Wavelength

t = Time duration of the laser pulse

U = Laser energy incident on the vacuum chamber window

Γ_v = Coefficient of reflection of the vanes

T_w = Coefficient of transmission of vacuum chamber window

ω = Angular velocity of suspension assembly

ω_o = Angular velocity of suspension assembly just before laser actuation

ω_s = Angular velocity of suspension assembly immediately after reflection of the pulse from the second vane

PE = Potential energy

KE = Kinetic energy

M = Mass of suspension assembly

V_y = Translational velocity of suspension in the direction of the incident laser beam

V_x = Translational velocity $\perp V_y$

S_y = Displacement of the c.m. of the suspension assembly in time T/4

Λ = Molecular mean free path

d = Molecular diameter

p = Pressure

N = Molecular density

V_{EN}= Entrance photocell voltages

V_{EX}= Exit " "

K = Attenuation between laser and entrance window of vacuum chamber

ACKNOWLEDGEMENTS

This report is based on a thesis submitted by the author to the University of Maryland in partial fulfillment of the requirements for the degree of M.S. in Physics.

I wish to thank my thesis advisor, Dr. Zaka I. Slawsky, for his guidance and encouragement in this work. I am particularly thankful to him for his theoretical assistance in interpretation of my results and for his general goal of trying to give a further insight into Physics to his students.

I appreciate the interest and contributions made by Prof. Karl F. Herzfeld, of Catholic University, through stimulating discussions with Dr. Slawsky and myself.

Special thanks are due to Dr. J. R. Dixon for his consultation time and advice which helped me considerably in the solution of important experimental problems.

I also wish to thank Mr. R. E. Grantham for his continued interest in this experiment and for his helpful suggestions concerning the instrument design.

Finally, I wish to acknowledge appreciation to the following members of the NOL Staff for cooperation in the use of equipment and facilities: P. R. Wessel, W. L. Clark, G. P. Worrell, C. A. Petersen, W. L. Ludwig, R. D. Johnson, J. L. Davis and D. L. Caskey.

CHAPTER I

INTRODUCTION

Less than two years after the first ruby laser was made to operate successfully by T. H. Maiman[1] in May 1960, the technological advances in this field resulted in increased laser energy outputs of two orders of magnitude. Maiman's laser had outputs ranging from several tenths of a joule to nearly one joule. By April 1962 one company[2] was offering a ten joule ruby laser with a future capability of fifty joules. A second company[3] was guaranteeing a ruby laser capable of thirty joules output. Further increases in laser output were being sought at that time and with the efforts being expended toward this goal, it appeared reasonable to assume that lasers of hundreds of joules of output could be expected. With such energies available having the properties of coherent plane waves, in addition to having high photon concentrations, an excellent means was presented for performing experiments on the interaction of electromagnetic radiation with matter.

In order to carry out a quantitative study of this nature, however, it would be necessary to measure the radiation used. The blackbody calorimeter, which had been used

satisfactorily, heretofore, was already being found to have serious drawbacks. Vaporization of the blackbody material and its associated decomposition resulted in measurement errors with usage[4]. Furthermore, by its principle of operation, the calorimeter absorbs the incident radiation making it impossible to use this radiation and simultaneously measure its energy.

It is generally agreed that the performance of high energy laser experiments should produce much useful information[5]. Some fundamental method, therefore, was sought for measuring the energy of a laser beam, without appreciably reducing this energy while permitting it to be simultaneously used in an experiment.

The idea of converting the photon momentum of a laser beam into mechanical momentum of a sensitive reflecting vane instrument appeared to be an ideal solution to this problem, since the laser beam could be made to enter and leave the instrument by reflection, and since a negligible amount of energy is absorbed by a good reflector. Furthermore, the total photon momentum, p, is proportional to the total beam energy, E. Thus, a measurement of total photon momentum is also a measure of the energy. This may be seen from the following relations beginning with

$$E = mc^2 \tag{1}$$

where c is the velocity of light, and m represents the associated photon mass. The total linear photon momentum in the beam is given by

$$p = mc \tag{2}$$

which leads to the relation between momentum and energy

$$p = E/c \tag{3}$$

The existence of radiation pressure was first predicted by J. C. Maxwell[6] in 1873 from mathematical studies of the stresses in an electromagnetic field. This was corroborated from thermodynamic principles by S. Bartoli[7] in 1876. Attempts to experimentally verify the Maxwell-Bartoli theory failed prior to 1901 because of inability to secure a sufficiently high vacuum. Gas effects resulted which were orders of magnitude greater than the radiation pressures sought. The first experiments giving indications of radiation pressure were described in 1901 by P. Lebedew[8] at the University of Moscow, and Nichols and Hull[9] at Dartmouth University. In 1924, J. D. Tear[10] combined the best features of the two earlier experiments and made a careful study of the factors contributing to gas effects[11]. He used this information to construct a torsion balance with the object of keeping gas effects to a minimum. However, he did not observe effects caused only by radiation pressure. At best, radiation pressure was indicated in his work by extrapolation

methods[12]. These experimenters were troubled by radiometer forces, spurious gas effects, and by the long time required for stabilization prior to making a measurement[13] with very sensitive torsion balance systems.

With the high photon concentrations available in pulsed laser beams, it appeared feasible to design an instrument which could be operated at reasonable vacuums with deflections due mainly to photon momentum, thereby making the instrument sensitivity predictable and repeatable. With these features the instrument would provide a means for making quantitative fundamental measurements of the momentum and energy in pulsed laser beams.

By employing a pair of vanes at 45 degrees to the incident beam instead of normal to the incident beam as previously done, it appeared that a couple could be produced thereby obtaining a maximum rotational effect. Furthermore, by applying this to a torsional ballistic pendulum system rather than a balance, the need for bringing the system to rest before making a measurement could be eliminated. Operation under conditions of initial oscillation appeared possible because it could be shown that the change in peak amplitude was proportional to photon momentum. (This is demonstrated in Chapter III, "Theory of Instrument Design" by the application of principles of conservation of momentum and energy.)

This experiment was, therefore, conceived to demonstrate that an instrument of sufficient sensitivity could be designed and built to convert the photon momentum of pulsed laser beams to readable mechanical deflections which would be proportional to the laser energy. As part of this experiment, energy measurements were also made for the purpose of comparison with a typical commercial calorimeter[14] of the type now used extensively for laser measurements. The difference found between these two methods suggests an interesting future problem for research which would be a detailed study of calorimetry problems and their solution leading to a satisfactory calorimeter for use with lasers.

In addition, the results obtained at the higher pressures although difficult to account for quantitatively, are very reproducible. This implies the existence of systematic gas effects in the free molecular flow regime not heretofore observed. This could well be a subject for future investigations.

CHAPTER II

APPARATUS AND EXPERIMENTAL PROCEDURE

1. <u>Description of momentum transfer instrument</u>. The instrument designed for this photon momentum experiment was a torsion ballistic pendulum shown diagrammatically in Fig. 1. A pair of reflecting vanes were mounted on a structure of fine aluminum tubing (0.91 mm outside diameter) and suspended from a ground glass joint at the top of the instrument by a gold suspension wire. This joint was rotatable and provided a means for initially positioning the reflecting vanes while the system was under vacuum. A galvanometer scale mirror for indicating deflections was fixed to a portion of the aluminum structure, which is shown in Fig. 1, attached to the lower end of the suspension wire. The vanes were hooked to the bottom of this tube after which the vacuum chamber cover and suspended vanes were lowered into position to complete the instrument. The suspension assembly was held together by vacuum wax melted by a warm soldering iron held close to the joints. A pair of entrance and exit windows were provided in the vacuum chamber to permit the laser energy to enter the chamber, undergo double reflection when the suspension was in the zero position, and

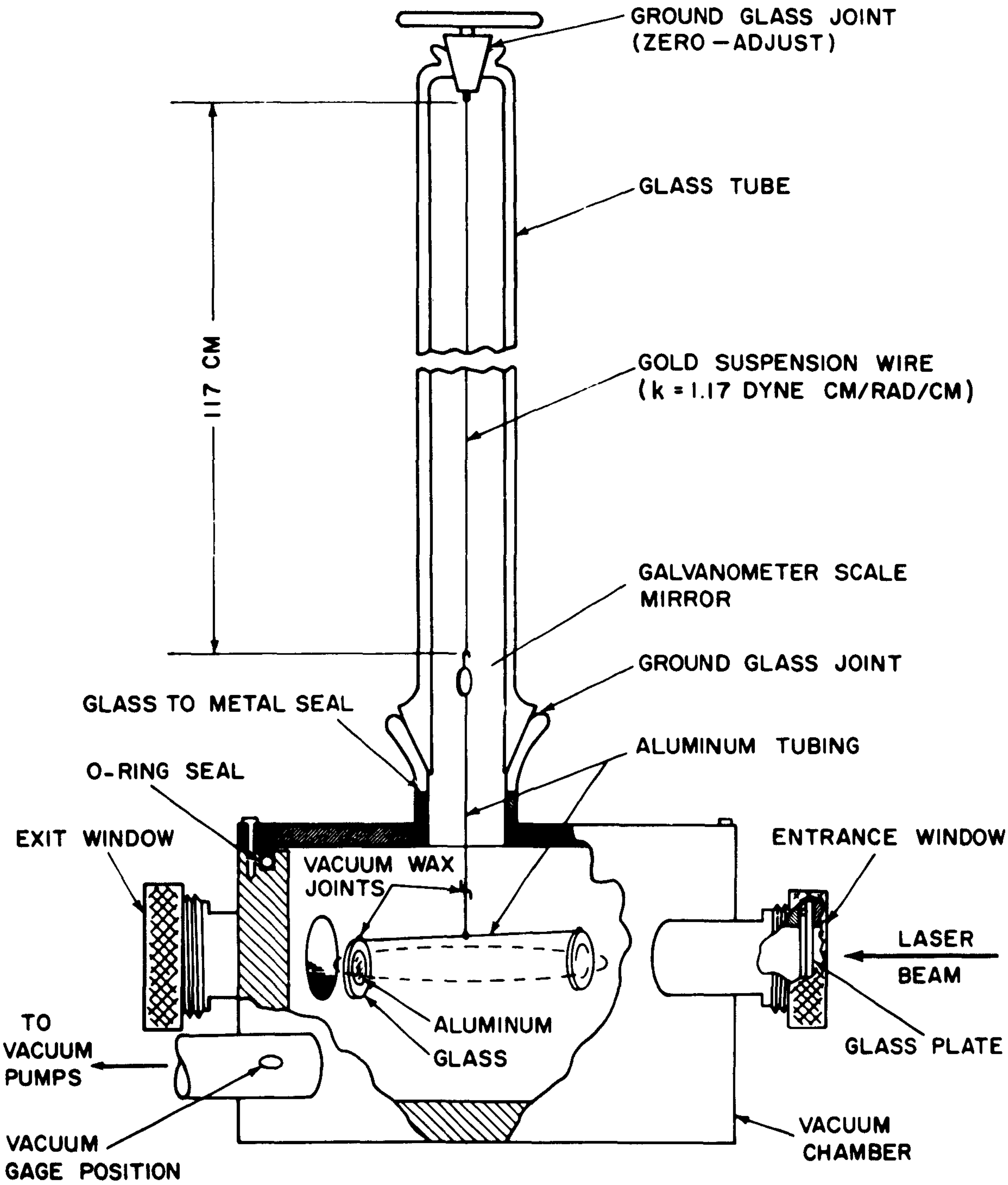

FIG. 1 INSTRUMENT FOR MOMENTUM CONVERSION

leave the chamber. This is shown more clearly in Fig. 2, an enlarged top view of the chamber. The suspension is shown in its zero position with the cross arm at right angles to the axes of the windows. The vanes were mounted at an angle of 45 degrees with the cross arm to produce the desired double reflection of the laser beam and to permit an impulse couple to be produced. This will be more fully explained in Chap. III, Theory of Instrument Design. The vanes were made by vacuum deposition of aluminum[15] on circular glass microscope cover slides (0.22 mm thick x 2.5 cm in diameter) and positioned on the suspension assembly so that the aluminized side received the incident laser energy as shown in Fig. 2. The object of this was to help reduce heating effects by presenting a surface of low absorbtion to the incident radiation thereby maintaining the front and back faces of the vane at nearly the same temperature to prevent the instrument from behaving as a radiometer.

To reduce possible interaction of the vanes with ambient magnetic fields due to the earth, or laboratory equipment, the vacuum chamber was made of magnetic material for shielding. Although the vanes and galvanometer scale mirror were made of aluminum on glass, the scale mirror was found to be slightly magnetic. Other experimenters[16] have noticed similar effects. This feature was taken advantage of by using a permanent

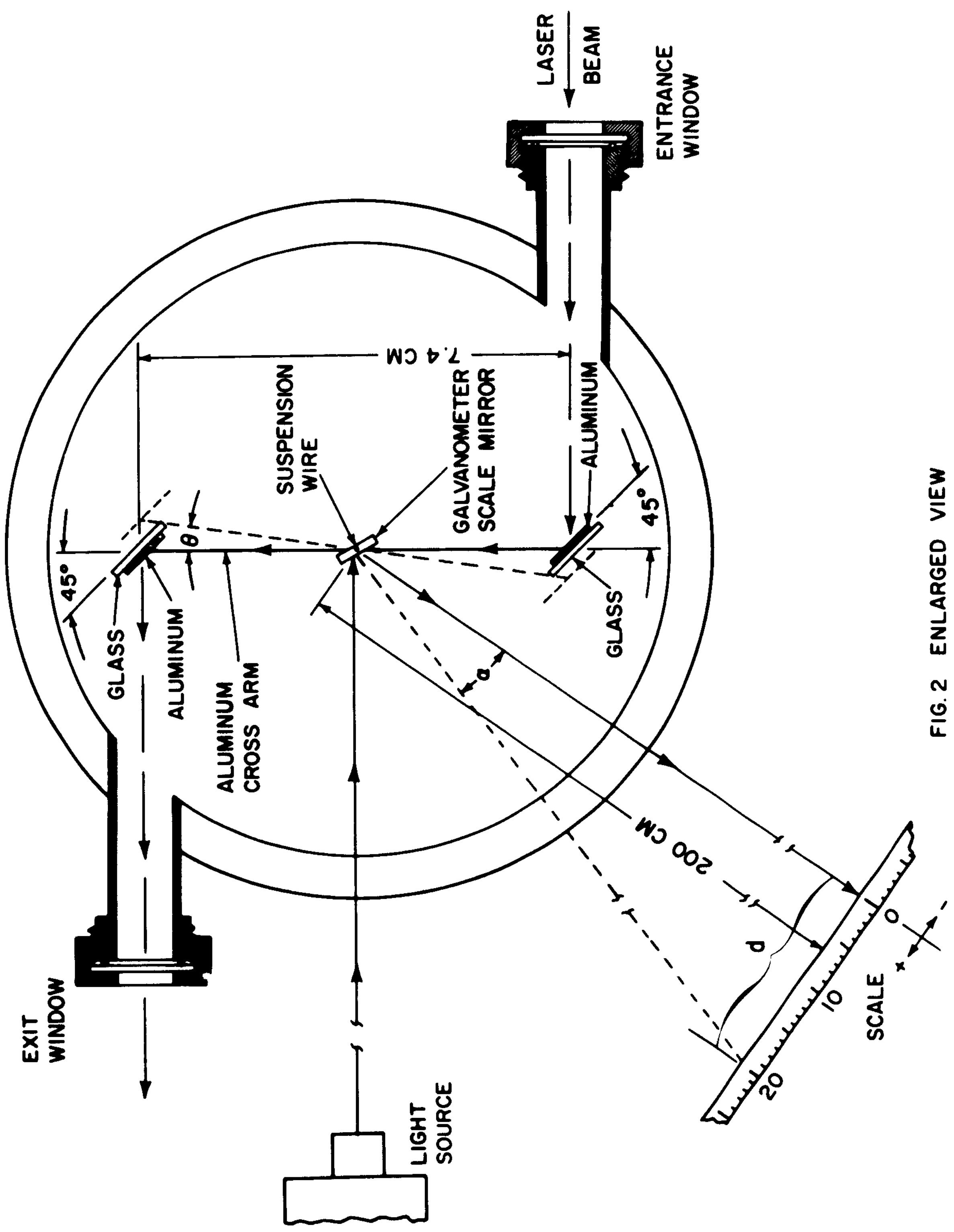

FIG. 2 ENLARGED VIEW

magnet to control the initial oscillations before taking data.[17] Shown in Fig. 2 are the galvanometer scale mirror, a conventional galvanometer light source aimed at this mirror and a scale upon which movement of the reflected scale indicator may be observed to indicate suspension position and deflection. The distance between the centers of the vanes was made the same as the distance between the window axes, shown in Fig. 2 to be 7.4 cm. The torque constant of the suspension wire was 1.17 dyne cm/rad, per cm of length of the suspension wire.[18] The suspension wire length, as shown on Fig. 2 was 117.0 cm. The distance from the scale mirror to the scale, 200 cm, is also shown on Fig. 2.

2. Over-all experimental setup. A diagrammatic sketch of the experimental setup is given in Fig. 3. The laser is shown emitting a pulse of energy which passes through a filter and collimator, a glass beam splitter, designated "entrance beam splitter", and the entrance window of the vacuum chamber to the first of the reflecting vanes. After reflection from both vanes it passes through the exit window and a second glass beam splitter designated "exit beam splitter." Fractions of the incident energy reflected from the beam splitters enter two photoelectric cells as shown in Fig. 3. The ground glass zero-adjust at the top of the instrument was adjusted to make the rest position of the

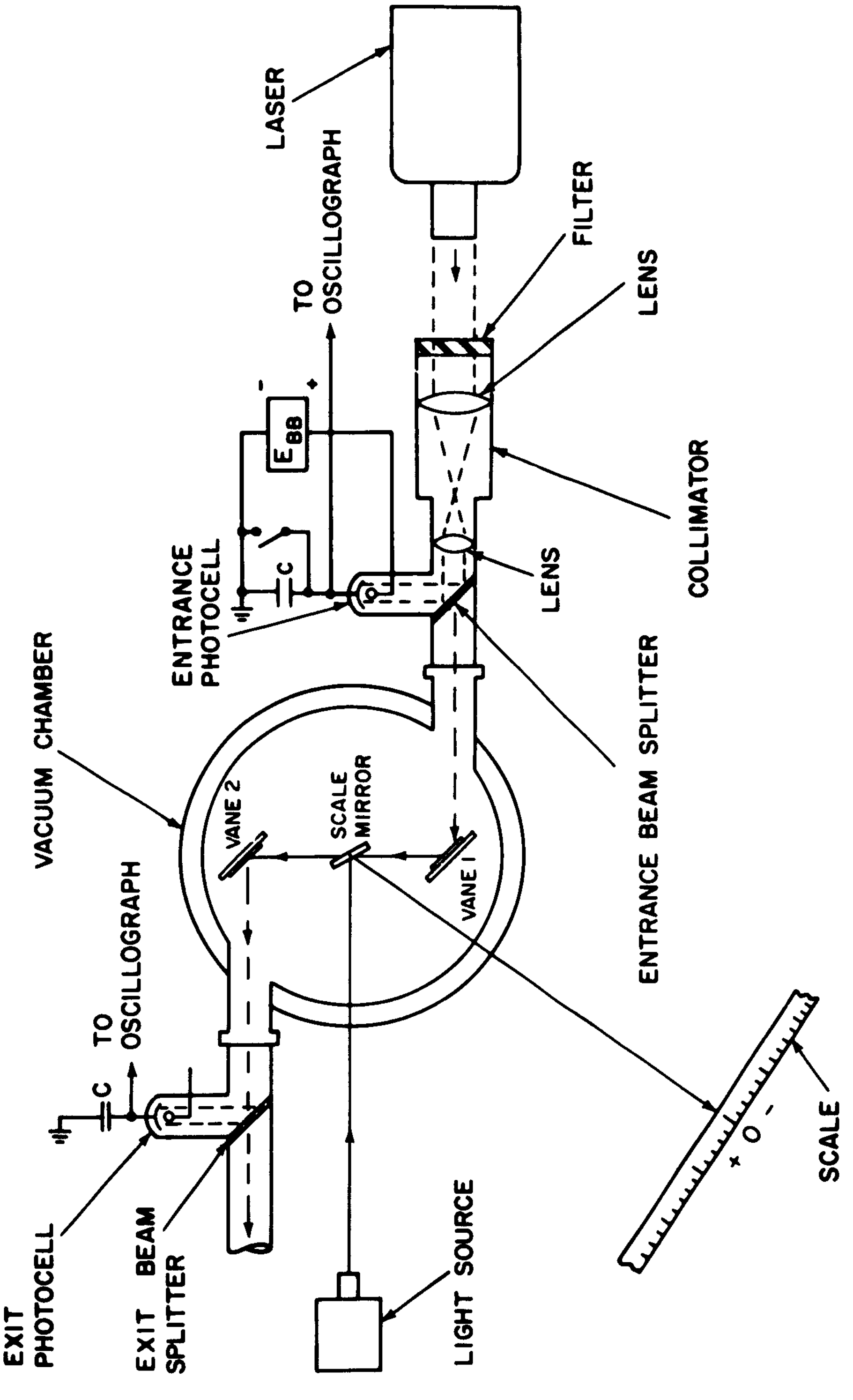

FIG. 3 EXPERIMENTAL SET-UP

suspension coincident with the zero position as shown in Fig. 3. This was done at atmospheric pressure to take advantage of air damping which prevented sustained oscillation of the suspension assembly, bringing it to rest in a relatively short time. With the suspension at rest, final orientation of the laser and collimator could be effected by sighting back through the exit window to the laser crystal. Next the scale light source was adjusted so that the hairline of its reflection lined up with the zero of the scale.

The voltages across the capacitors, C, were recorded, with each laser fire on a two channel Sanborn Pen oscillograph model No. 322. The oscillograph may be seen in Fig. 4, a photograph of the experimental setup, which also shows the suspension zero, glass tube, vacuum chamber and scale of the instrument. The glass tube was painted with an electrically conducting paint which was grounded to prevent static charge effects. The laser head, console, capacitor bank and Dewar of the laser[19] used in this work may also be seen in Fig. 4, as well as the photocell power supply and one of the clock timers used to plot deflection versus time of the suspension system.

Figure 5 is a close-up photograph of the experimental setup showing the instrument mounted on an optical bench. It was connected to the vacuum system by a ground glass

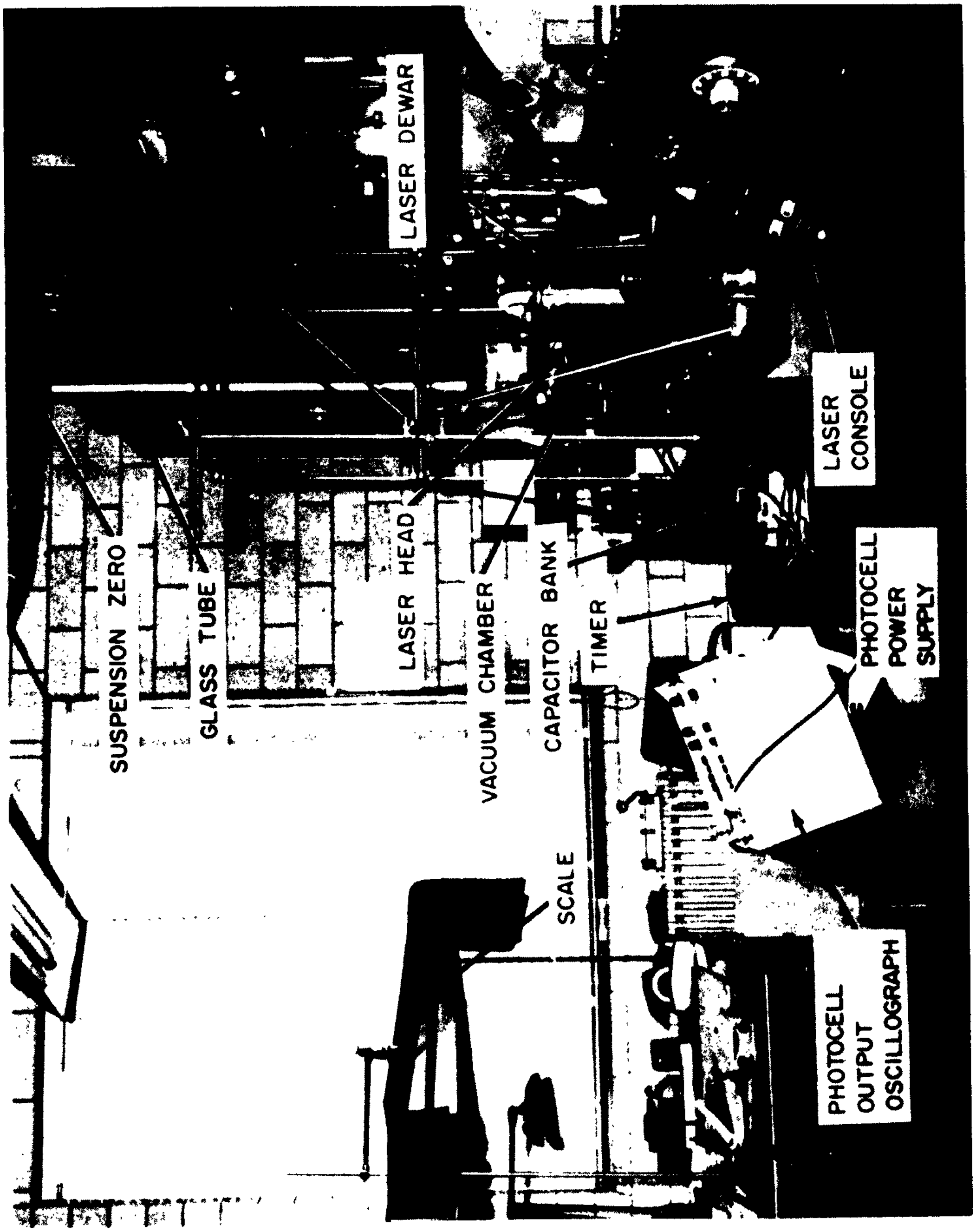

FIG. 4 PHOTOGRAPH OF EXPERIMENTAL SETUP

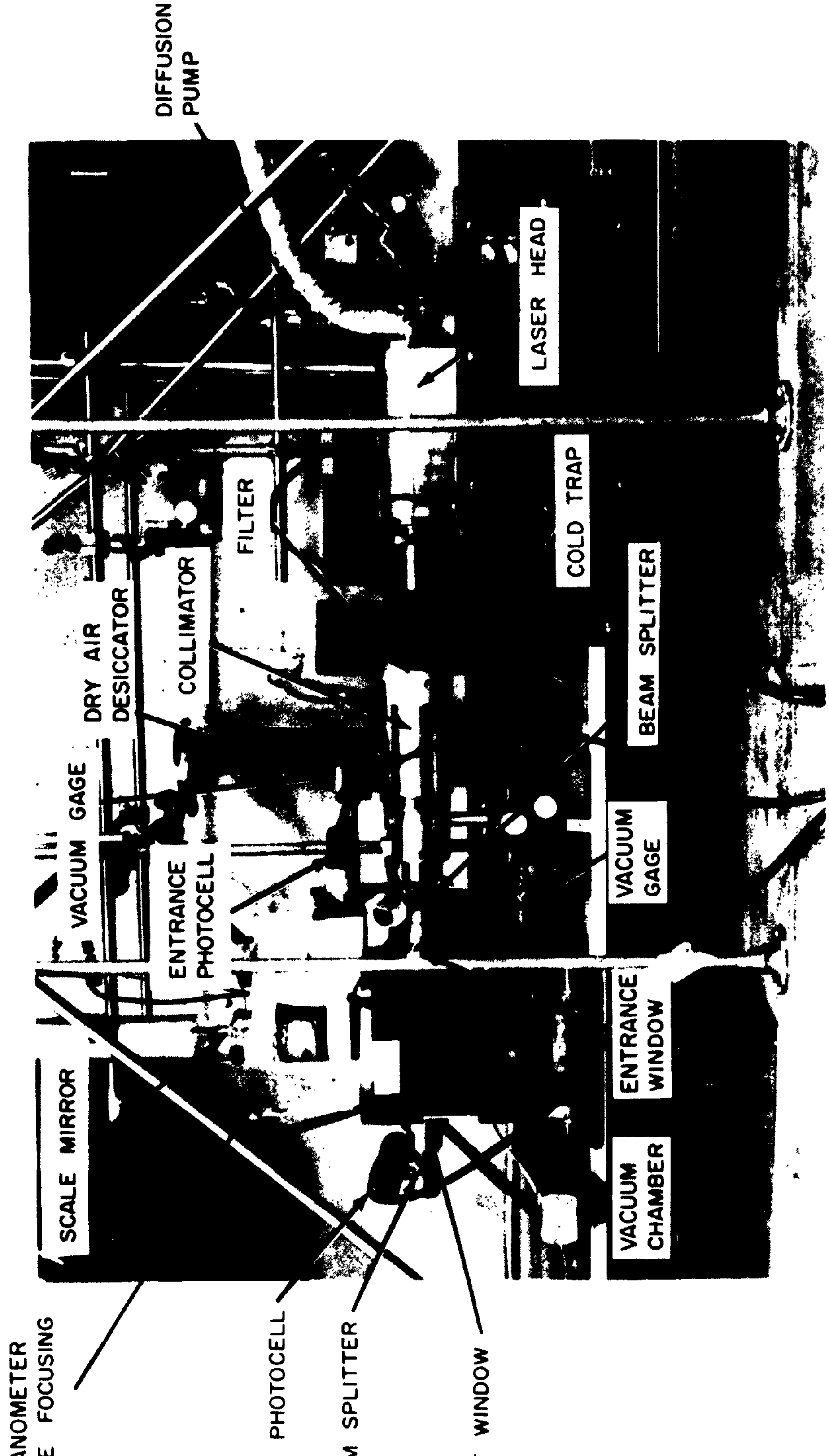

FIG. 5 CLOSEUP OF EXPERIMENTAL SETUP

spherical joint to permit final orientation. Components of the vacuum system were a fore pump which is not shown, an oil diffusion pump, a liquid nitrogen cold trap and two vacuum gages of different pressure ranges. The higher range gage served the purpose of indicating when the proper operating range of the diffusion pump had been reached, and the low pressure gage, a Phillips gage, was used for the pressure measurements in the experiment. The collimator was made of two aluminum tubes which were threaded for adjustment of the distance between two convex lenses as shown schematically in Fig. 3. The focal lengths of the two lenses were 112 mm and 67 mm, resulting in a reduction in laser beam cross section of approximately 0.6. In this way, it was assured that the entire laser beam would be incident on the vanes. The filter was a No. 70 Kodak, Wratten filter for attenuating the shorter wavelengths of the Xenon flash lamp output below the laser wavelength of 6943 A. The beam splitters were uncoated glass microscope slides ground to the shape of the holders, and the photocells were RCA type 925 with the S-1 sensitivity surface.

The commercial calorimeter[20] used in the experiment was a blackbody thermocouple type. The blackbody was contained in an evacuated glass chamber with a focusing lens as the front window. To determine the energy of incident radiation on the calorimeter, the thermocouple output, in microvolts,

was multiplied by 0.12 joules per microvolt, the constant determined for this calorimeter. The calorimeter parameters were obtained[21] and the value of the constant was checked.

3. Measurement procedure. The system was evacuated to a point where damping of the oscillations was negligible (10^{-5} mm of Hg) and measurements of the period of oscillation were made in order to check the manufacturer's value of the torque constant of the suspension wire. A comparison of this value with the calculated value was then made. The moment of inertia used in this calculation was calculated from the masses and dimensions of the suspension components measured during assembly.[22]

The next step in the procedure was to determine the pressure below which deflections of the suspension system would be due to photon momentum of the laser beam with negligible contributions from radiometer effects due to vane heating. Since radiometer effect is pressure dependent, the object of this portion of the procedure was to find the pressure region where deflection changes were not pressure dependent. The pressure was stabilized at values giving molecular mean free paths greater than the suspension dimensions as calculated in Chap. III. At each pressure the initial oscillations of the suspension were recorded for several cycles, and then after each laser fire in a sequence of laser fires to

be more fully described. The major difficulty in past use of sensitive torsion balance systems, that of trying to zero the instrument before taking a measurement[23], was solved by the following procedure: The peak amplitudes of the initial oscillations were recorded with at least two maxima and two minima being taken. In addition to reading the peaks, intermediate readings of deflection were also recorded with measurements of time elapsed between readings made with a pair of stop clocks. It was thus possible to plot the oscillations against time so that any deviations from normal harmonic oscillation due to external causes, such as building vibrations, could be detected. Typical plots of the oscillations observed are shown in Figs. 11A and 11B (Chap. IV, Results and Discussion) in which the horizontal tangent lines are the observed maxima and minima. The laser was first fired as the suspension and the scale indicator passed through the zero position rotating in the positive direction; i.e., toward the position shown in dashed lines in Fig. 2. At laser fire, indicated in Fig. 11A by "1st Fire," the clocks were started from zero. As previously described, the entrance and exit photocell outputs were recorded on the Sanborn Oscillograph, Fig. 4. The suspension oscillations were recorded after the laser fire for two cycles while the laser was brought to the same conditions of ruby crystal temperature and capacitor bank

voltage for the next fire. As the suspension crossed the zero position in the negative direction, the laser was fired to give the "2nd Laser Fire" as indicated. In the pressure region where no spurious gas effects were present, this procedure was continued for at least six laser fires at the pressures investigated. The attempt was made to reproduce the laser output energy for all laser fires in obtaining these data on deflection as a function of pressure. To minimize errors in peak measurements due to damping, it was desirable to fire the laser on the next zero crossing of the desired direction after the two cycle oscillation data had been recorded. The effect of laser fire on deflection was observed at pressures of 5.2×10^{-4}, 3.4×10^{-4}, 8.2×10^{-5}, 4.5×10^{-5}, and 10^{-5} mm of Hg. In the low pressure region[24] data was taken at pressures of 8.2×10^{-5}, 4.5×10^{-5} and 10^{-5} mm of Hg to see if deflection remained constant independent of pressure, as expected, where deflection is due mainly to photon momentum. At the higher pressures, where the mean free path was $\approx$ the dimensions of the system, the foregoing procedure required modification at the second laser fire. Instead of firing as soon as possible, a long enough time was permitted to elapse after the first laser fire to permit temperature stabilization in the vacuum chamber. (This condition was reached when gas effects were no longer observed

to shift the zero of oscillation). The resulting oscillation was then recorded as the "initial oscillation" for the second laser fire. To obtain the deflection at these pressures, the oscillation data obtained from three laser fires were averaged. A typical oscillation curve obtained in the higher pressure region[25] is shown in Fig. 12.

The next step in the measurement procedure was to stabilize at a pressure in the low pressure region to see if deflection was proportional to laser energy in accordance with the sensitivity calculations of Chap. III. The output energy of the laser was varied from threshold to maximum, with a relative measure of energy being given by the photocell outputs. Peak deflections of the suspension, as well as data for plotting the oscillations, were recorded before and after each laser fire. It should be noted that an important part of this procedure, in varying the output of the laser, was to charge the capacitor bank of the laser to the same value for each fire, thus maintaining the xenon optical pump energy constant. The varying laser output was obtained by controlling the flow rate of the coolant thereby to vary the temperature of the laser crystal. The laser fires were made in pairs with the suspension rotating first

in the positive, then in the negative direction[26], the laser energies for each pair being duplicated as closely as possible. Included in these data were measurements at full optical pump energy, but below laser threshold[27] to see if any deflection could be observed when laser action did not take place in the ruby crystal.

Table I. Coefficients of transmission and reflection of optical components

Component	Angle of incidence	Coefficient of reflection	Coefficient of transmission
Reflecting vane	45°	0.753	0
Collimator	0°	--	0.80
Entrance beam splitter	45°	0.034	0.865
Exit beam splitter	45°	0.023	0.830
Vacuum chamber window	9°	0.072	0.922
No. 70 Filter (at λ = 6943A	9°	--	0.71

Measurements of the coefficients of reflection and transmission[28] of the optical components of the system were made and the results of these measurements are given in Table I in which the coefficient of reflection is defined as the ratio of the radiant energy reflected to the incident radiant energy. The coefficient of transmission is defined as the ratio of the radiant energy transmitted to the incident

radiant energy. A plot of the response of the No. 70 Kodak Wratten filter is given in Fig. 6.

Calibration of the Phillips vacuum gage was performed on a vacuum system using a McLeod gage as a standard[29]. The calibration curve is shown in Fig. 7.

To compare the energy measurements made by the torsion pendulum instrument with the calorimeter, the collimator and photocell assembly, shown in Fig. 3, were aligned with the calorimeter so that the blackbody was in the same relative position as vane 1. The laser was fired at temperatures from 120°K to room temperature and measurements of photocell output vs energy obtained from the calorimeter readings were recorded. Sufficient time between laser fires was allowed to elapse for the calorimeter to become stabilized. This was approximately thirty minutes. The curve of photocell output vs energy indicated by the calorimeter is shown in Fig. 8.

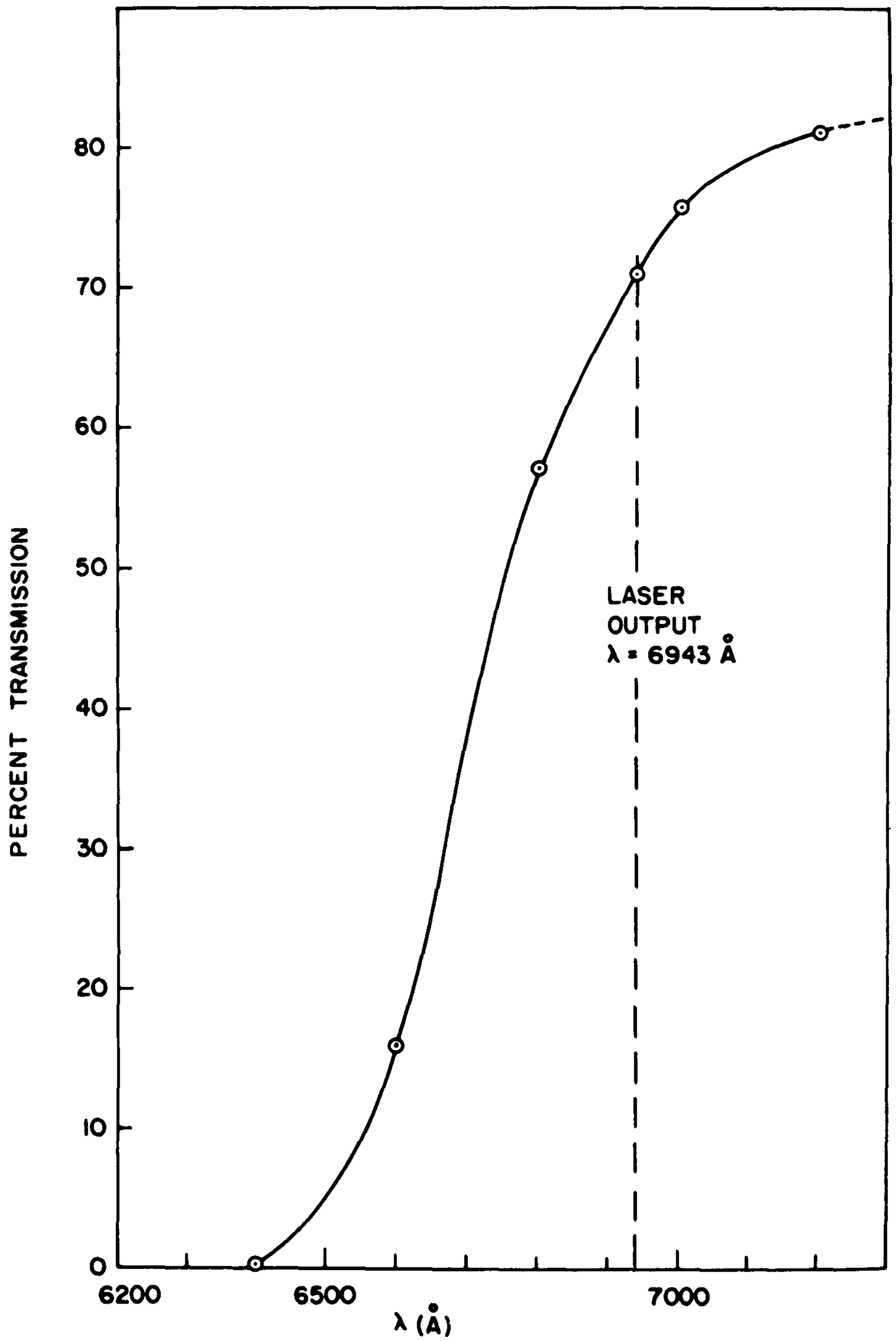

FIG. 6 MEASURED TRANSMISSION VERSUS WAVE LENGTH OF #70 KODAK WRATTEN FILTER

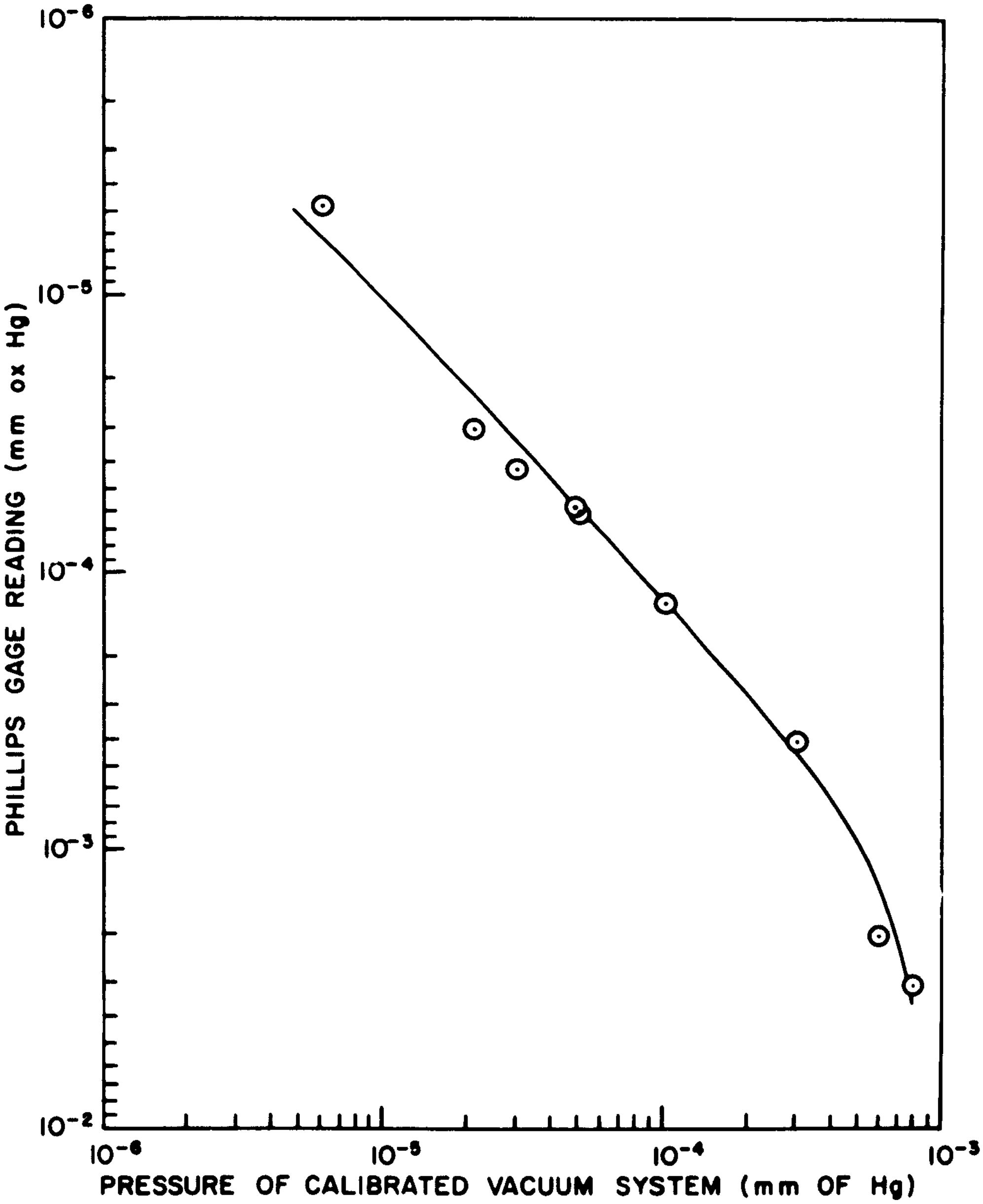

FIG. 7 PHILLIPS VACUUM GAGE CALIBRATION — McLEOD GAGE USED AS STANDARD

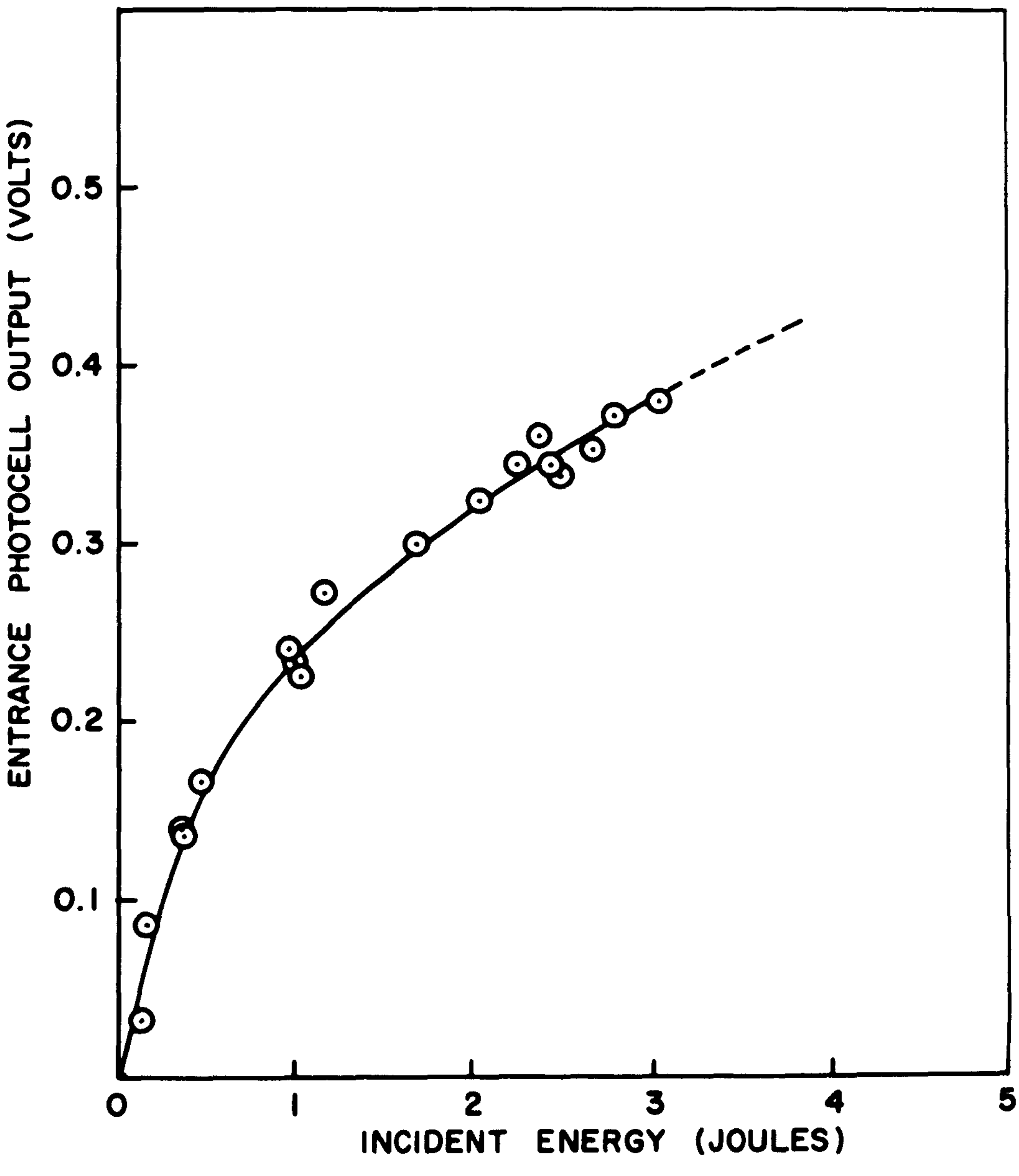

FIG.8 ENERGY CALIBRATION OF ENTRANCE PHOTOCELL USING CALORIMETER AS REFERENCE

CHAPTER III

THEORY OF INSTRUMENT DESIGN

1. Two vane design. Since the desired object in this experiment was to transfer the linear photon momentum of a laser beam into angular momentum of the suspension system of a torsion pendulum instrument, it was desirable to obtain a maximum of rotation with a minimum of translation. The idea of a pair of reflecting vanes was therefore employed. The vanes were fixed at an angle of 45° to the cross arm, as shown in Fig. 2. In the rest position, shown by the solid lines, incident light energy was reflected from the vanes with an exit direction parallel to the incident direction. This was to provide an impulse couple about the axis of the suspension wire as will be described in greater detail. With this arrangement, it was not necessary to constrain the center of mass (c.m) of the suspension from the bottom of the instrument. This feature provided greater sensitivity.

2. Ideal case. Consider first the ideal case of $\Gamma_V = 1$ (perfect vane reflectivity equal to unity), an initially stationary suspension in the zero position, as shown in Fig. 2, and no gas effects. Assume a pulse of electromagnetic

energy, U, such as the output of a pulsed ruby laser, of short time duration t. If $t \ll T/4$, where T is the period of oscillation of the suspension system, then the suspension position will remain essentially unchanged for the duration of the laser pulse. The total linear momentum, p, of the photons in the laser beam before reflection from the first vane may be obtained by substitution into Eq. (3) giving

$$p = U/c \qquad (4)$$

where c is the velocity of light in vacuum. Since the mass of the vane is >> the equivalent mass of the photon, the recoil momentum of the photon must be very nearly the same as the incident momentum. For $\Gamma_v = 1$ there is no loss on reflection and the <u>total</u> photon momentum before and after each reflection is also given by (4). By summing the components of momentum in the initial beam direction and the components normal to it (along the cross arm) it will be seen that the suspension will acquire no translational component of momentum. The total angular momentum, $I\omega$, of the suspension about the axis of the suspension wire, immediately after reflection of the pulse from the second vane, may be found by applying the principle of conservation of angular momentum to the laser beam and the suspension

system. This results in

$$pR = I\omega - pR \tag{5}$$

where I is the moment of inertia of the suspension about the axis of the suspension wire, ω is the angular velocity of the suspension immediately after the beam leaves the second reflector, and R is the distance from the axis of the suspension wire to the centers of the reflecting vanes. Substitution of Eq. (4) into (5), and rearranging terms results in

$$I\omega = 2RU/c \tag{6}$$

If θ is the peak rotation of the suspension from the zero position, then the potential energy, PE, stored in the suspension wire at deflection θ is given by

$$PE = \tfrac{1}{2}k\theta^2 \tag{7}$$

where k is the torque constant of the suspension wire. The kinetic energy, KE, of the suspension, immediately after the laser pulse has passed the second vane, may be written as

$$KE = \tfrac{1}{2}I\omega^2 \tag{8}$$

If there are no frictional losses in the suspension wire and no losses due to air damping, then by application of the principle of conservation of energy,

$$PE = KE \tag{9}$$

and by substitution of (7) and (8) into (9) one obtains

$$\tfrac{1}{2}k\theta^2 = \tfrac{1}{2}I\omega^2 \tag{10}$$

$$k\theta^2 = (I\omega)^2/I$$

$$I\omega = \theta(kI)^{\frac{1}{2}} \tag{11}$$

Substitution of Eq. (11) into (6), and solving for θ results in

$$\theta = 2RU/c(kI)^{\frac{1}{2}} \tag{12}$$

Equation (12) shows that the angular deflection of a torsion pendulum, of the type herein described, is proportional to the energy of a short time duration pulse. The more general case will be considered next.

3. General case. Consider the more general case, shown diagrammatically in Fig. 9, of vane reflectivity equal to some value, Γ_v, with initial suspension rotation about the c.m., shown at S. There is no initial translation of the c.m., and gas effects due to vane heating are assumed to be negligible. Air damping is also assumed negligible. The position of the suspension, as shown in Fig. 9, is both the zero position and the center of oscillation. A short pulse of laser energy, U, is assumed to pass through a vacuum chamber window having a coefficient of transmission, T_w when the suspension is in the position shown in Fig. 9. The energy incident on vane 1 will be T_wU with a photon momentum, T_wUR/c, about the axis of the suspension wire.

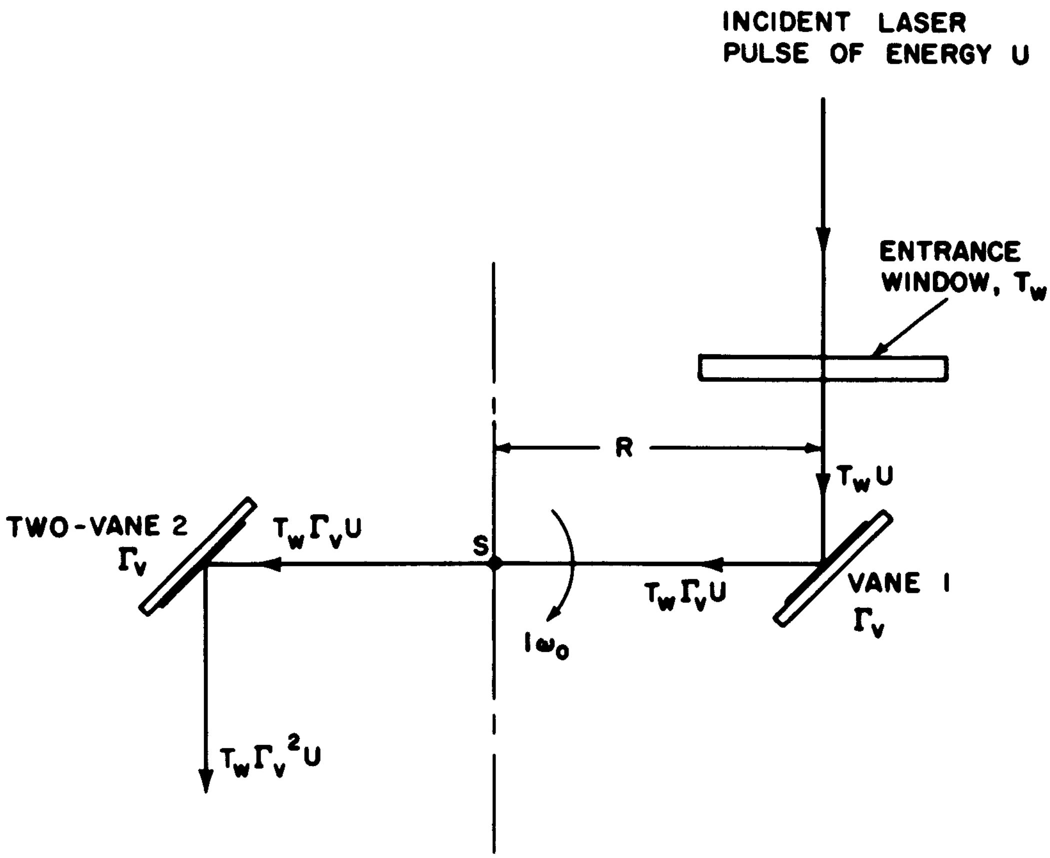

FIG.9 SCHEMATIC OF TWO VANE TORSION PENDULUM

(The clockwise direction as viewed in Fig. 9, will be taken as positive). If $I\omega_o$ represents the initial angular momentum of the suspension on crossing the zero position, and $I\omega_s$ represents the resulting angular momentum of the suspension immediately following a laser fire, then application of the principle of conservation of angular momentum results in

$$I\omega_o + T_w UR/c = I\omega_s - T_w \Gamma_v{}^2 UR/c \qquad (13)$$

Rearranging terms gives

$$I\omega_s - I\omega_o = (1 + \Gamma_v{}^2)\ T_w RU/c \qquad (14)$$

where $(I\omega_s - I\omega_o)$ represents the difference between the initial angular momentum on zero crossing just before laser fire, and the angular momentum on zero crossing just after laser fire, i.e. immediately after reflection of the energy from vane 2. By application of energy conservation principles and following the procedure used in going from Eq. (6) to Eq. (12), one finds that Eq. (14) may be written in the form

$$\theta_s - \theta_o = (1 + \Gamma_v{}^2)\ T_w RU/c(kI)^{\frac{1}{2}} \qquad (15)$$

where θ_o represents the peak angular deflection of the suspension before laser fire, and θ_s represents the peak angular deflection after laser fire. It should be noted that Eq. (15) shows that the <u>difference</u> in peak angular deflections of the suspension is directly proportional to the laser energy <u>irrespective of the initial oscillation</u> of the suspension.

one obtains

$$MV_x = (T_w\Gamma_v U/c) - (T_w\Gamma_v U/c) \ . \tag{20}$$

Solving Eqs. (19) and (20) for V_y and V_x respectively gives

$$V_y = T_w U \quad (1 - \Gamma_v{}^2)/Mc \tag{21}$$

and

$$V_x = 0 \tag{22}$$

This indicates that translational motion only in the direction of laser beam incidence may result. For the case where $\Gamma_v = 1$, Eq. (21) reduces to

$$V_y = 0 \tag{23}$$

with no translational motion as previously indicated. Also, for $\Gamma_v = 1$, Eq. (18) reduces to $\theta_s = \theta$, as would be expected.

It will be shown in the next section that the translational motion described in Eq. (21) is negligible compared to the scale deflections observed.

4. Scale readings. The angular deflections, θ_o and θ_s in Eq. (15) have corresponding linear deflections d_o and d_s which are read on the scale by the galvanometer scale mirror arrangement. (Refer to Fig. 2). For a deflection θ we have, from Fig. 2,

$$\alpha = 2\theta \tag{24}$$

where α is the angle through which the reflected scale light rotates for the suspension rotation, θ. If the distance

from the scale to the scale mirror is represented by D, then the deflection, d, on the scale may be written

$$d = D \tan \alpha \tag{25}$$

and

$$d = D \tan 2\theta \tag{26}$$

For small angles[30] of deflection, Eq. (26) becomes

$$d = 2\theta D \tag{27}$$

which, when applied to the angular deflections θ_s and θ_o, leads to

$$\theta_s = d_s/2D \tag{28}$$

and

$$\theta_o = d_o/2D \tag{29}$$

Substitution of Eqs. (28) and (29) into Eq. (15) gives

$$d_s - d_o = 2(1 + \Gamma_v^{\,2})T_w RDU/c\ (kI)^{1/2} \tag{30}$$

This result indicates that the difference in the peak deflections, $(d_s - d_o)$, before and after laser fire, is proportional to laser beam energy, U, regardless of the initial deflection, d_o. This difference may be positive or negative in sign depending on the initial direction of rotation of the suspension system when the laser is fired. For a positive direction of suspension rotation, i.e. vane 1 (Fig. 9) moving away from the laser, there should be an increase in peak deflection, and $(d_s - d_o)$ should be positive.

For the case of vane 1 moving toward the laser at fire, i.e. negative rotation, the quantity (d_s - d_o) should be negative, but of the same magnitude for the same laser energy. It was this result that indicated that a sensitive torsion pendulum could be used for this experiment in the manner described in the Measurement procedure section of Chap. II.

5. Instrument sensitivity calculations. The sensitivity of this instrument will be defined as the linear change in peak deflection (cm), as read on a scale D (cm) from the suspension wire, per unit of incident pulse ot energy (joules). The sensitivity of the instrument used in this experiment may be calculated by substituting the values of the physical characteristics of the instrument into Eq. (30). These values are listed in Table II.

TABLE II. Physical characteristics of the torsion pendulum instrument

Physical Characteristics of Instrument	Value
Moment of inertia[31]	7.75 gm cm^2
Torque constant [32, 33]	1.00 x 10^{-2} dyne cm/rad
Distance between vane centers (2R)[34]	7.40 cm
Distance of scale from suspension[35]	200. cm
Coefficient of transmission of window	0.92
Coefficient of reflection of vane[36]	0.75
Mass of suspension[37]	0.98 gm

Upon substitution of the values given in Table II, assuming an energy of one joule, and using $c = 3 \times 10^{10}$ cm/sec, the sensitivity obtained is

$$d_s - d_o = 2.55 \text{ cm/joule} \tag{31}$$

The effect of the translational motion may also be determined by substitution of the appropriate values from Table II into Eq. (21). Solving for the velocity of translation, for a laser pulse of 1 joule, results in

$$V_y = 1.37 \times 10^{-4} \text{ cm/sec} \quad . \tag{32}$$

The time required to make a measurement of the first peak deflection of the suspension is T/4 where T is the period of oscillation. The displacement, S_y, of the c.m. in this time, moving at the velocity given in Eq. (32), may be calculated from

$$S_y = V_y T/4 \quad . \tag{33}$$

The period for this instrument was found to be 175 seconds. Substitution of this value of the period, and the value of V_y given in Eq. (32), results in

$$S_y = 6.0 \times 10^{-3} \text{ cm/joule} \quad . \tag{34}$$

This displacement is negligible compared with the scale reading of 2.55 cm/joule as given in Eq. (31). Therefore, translational effects may be neglected with the use of this instrument.

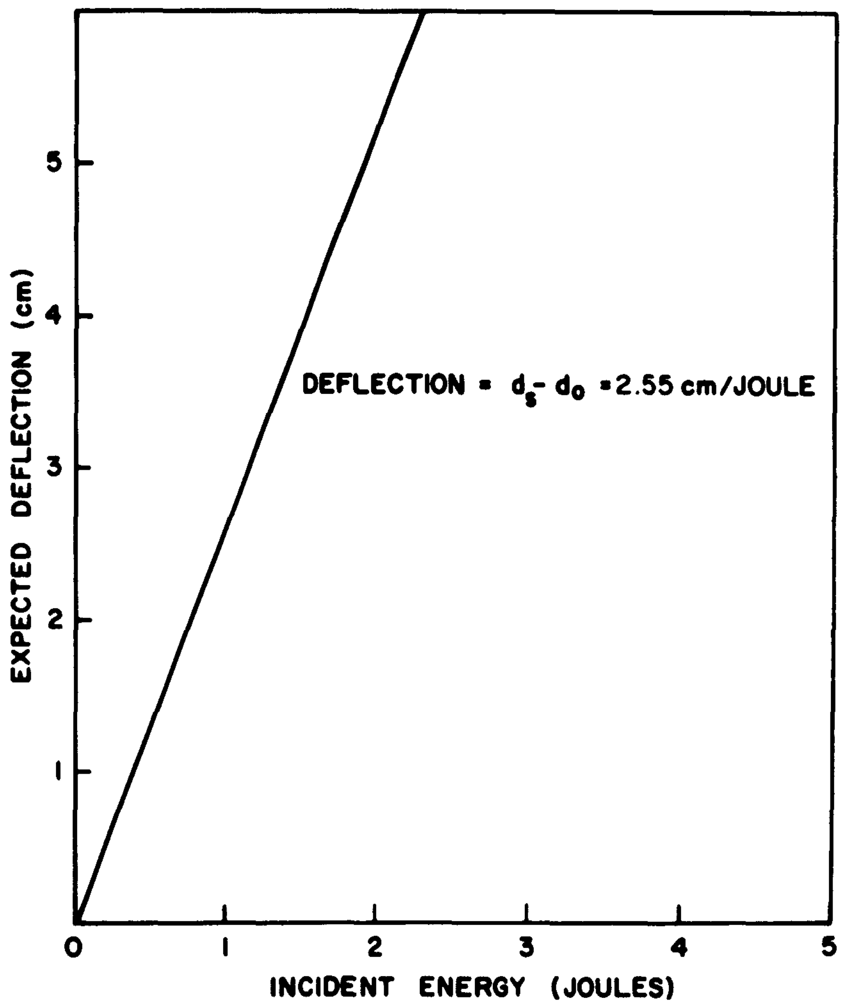

FIG.10 CALCULATED SENSITIVITY CURVE OF INSTRUMENT — EXPECTED DEFLECTION VERSUS INCIDENT ENERGY

This was borne out experimentally. For scale deflections in the order of 5 cm, no translational effec+s could be observed. Thus, Eqs. (30) and (31) are valid and give the instrument sensitivity. The instrument sensitivity curve is given in Fig. 10, and the calculations of Eqs. (31), and (32) are shown in Appendix B.

6. Choice of vane separation. Because of the double reflection of the laser beam by the two vanes of the instrument it was desirable, for practical considerations, to have the entrance and exit-window axes (see Figs. 2 and 3) separated by a distance of at least 5 cm. It was, however, desirable to have the vacuum chamber sufficiently small so that a reasonable vacuum would be sufficient to reach the region where gas effects become small compared to momentum effects. This should begin to occur where the molecular mean free path is of the order of the vacuum chamber dimensions[38]. The equation for the mean free path, Λ, is given by[39]

$$\Lambda = 1/N\pi d^2 \qquad (35)$$

where N represents the number of molecules per cm^3 and d represents the molecular diameter which may be taken approximately equal to 3.1×10^{-8} cm. To find the pressure, P, necessary in the vacuum chamber to attain a mean free path

of the diameter of the chamber ($\approx$15 cm), the value of N from Eq. (35) is found to be

$$N = 2.2 \times 10^{13} \text{ molecules/cm}^3 \quad . \tag{36}$$

Since molecular density is directly proportional to pressure, one may write

$$P/P_{atm} = N/N_{atm} \tag{37}$$

where P_{atm} is atmospheric pressure (760 mm of Hg) and N_{atm} is the molecular density at STP which is $\approx 2.7 \times 10^{19}$ molecules/cm^3. Substitution into Eq. (37) yields

$$P = 6.2 \times 10^{-4} \text{ mm of Hg} \quad . \tag{38}$$

The value of pressure given in Eq. (38) represents the pressure at which gas effects should begin to disappear. Thus, with an instrument of this size the required pressures appeared reasonable,[40] with the pressure range to be investigated expected to be between 10^{-3} and 10^{-6} mm of Hg. The results which were obtained agree with this. These results are discussed in Chap. IV.

7. Suspension torque constant. The suspension torque constant, k, was calculated from the manufacturer's value and the measured length of the suspension wire. It was found to be $1.17/117.0 = 1.00 \times 10^{-2}$ dyne cm/rad. This value was checked by calculating the period of the system which is given by

$$T = 2\pi(I/k)^{\frac{1}{2}} \quad . \tag{39}$$

Substitution of the calculated value of moment of inertia, 7.75 gm cm^2 (Appendix A) and the above value of k into Eq. (39) resulted in a calculated period of 174.7 seconds. This compared remarkably well with the observed period of 175 ± 1 seconds, verifying that the manufacturer's value was correct.

It might be interesting to note that this instrument would give a deflection of one radian for a pressure differential of the order of 10^{-3} dynes/cm^2, or 10^{-6} mm of Hg, on opposite surfaces of the vanes.

CHAPTER IV

RESULTS AND DISCUSSION

1. Introduction. Readable deflections of the momentum transfer instrument were observed in this experiment. At pressures below 5 x 10^{-5} mm of Hg, these deflections appeared to be due mainly to the photon momentum of a pulsed laser beam. The observed deflections were repeatable within the accuracy of the experiment. In a series of laser fires, with alternately positive and negative initial rotation of the suspension, the changes in peak deflection were equal. This was the necessary condition for deflection to be due to momentum as shown in Sec. 4 of Chap. III, Theory of Instrument Design. The procedure is described in Sec. 3 of Chap. II. Verification was made that contributions to deflections in the momentum region were not due to gas effects of small time duration. This was done by observing instrument deflections over a pressure range in which the dependency of deflection on pressure disappeared as the pressure was reduced. As an additional cross-check, deflections at the lowest required pressure, 10^{-5} mm of Hg, were observed for two values of

initial peak deflection. These results experimentally verified Eq. (30), the instrument sensitivity relation of Chap. III.

The experimental results which were related to the effect of pressure on deflection will be presented in two parts, as "Low pressure results" and "Higher pressure results". The low pressure results are for the data taken at pressures of 10^{-5}, 4.5×10^{-5}, and 8.2×10^{-5} mm of Hg. These results constitute the major part of the data to be presented and discussed. The higher pressure results are for the data taken at 3.4×10^{-4} and 5.2×10^{-4} mm of Hg, and are presented here to indicate how the low pressure region was determined for performing this momentum transfer experiment.

In Sec. 6 of Chap. III, a calculation was made of the pressure corresponding to a molecular mean free path of 15 cm, the diameter of the vacuum chamber. This pressure, at which gas effects should begin to disappear, was found to be 6.2×10^{-4} mm of Hg. At a pressure just below this (5.2×10^{-4} mm) definite gas effects were observed. The pressure was then lowered to look for momentum effects and the pressures, given above, were investigated.

It should be noted that it is sometimes assumed[41] that operation at mean free paths of the order of the instrument

dimensions will give results free of gas effects. Our results indicate, however, that experimental verification is required in experiments of this nature.

2. Low pressure results. A typical plot of the observed instrument suspension oscillations, in the low pressure region, is given in Figs. 11A and 11B. The pressure was 10^{-5} mm of Hg, and the initial peak amplitudes were relatively large. As shown, the first two cycles represent the initial oscillation before laser fire, having amplitudes of + 42.4 cm and - 43.2 cm. The first laser fire was triggered as the suspension crossed the zero position while rotating in the positive direction (vane 1, Fig. 9, moving away from the laser). An increase in peak deflection resulted with the new peak values of +47.1 cm and -48.4 cm. This calculates out to an increase of 5.0 cm, obtained by averaging the positive and negative peak changes. The values of "V_{EN}" and "V_{EX}" in Figs. 11A and 11B represent the integrated output voltages of the entrance and exit photocells respectively (see Fig. 3). The second laser fire occurred as the suspension crossed zero in the negative direction. A reduction in peak amplitude resulted with the new peak values of +42.1 cm and -43.4 cm. This corresponded to a change in peak deflection of -5.0 cm, and reestablished the

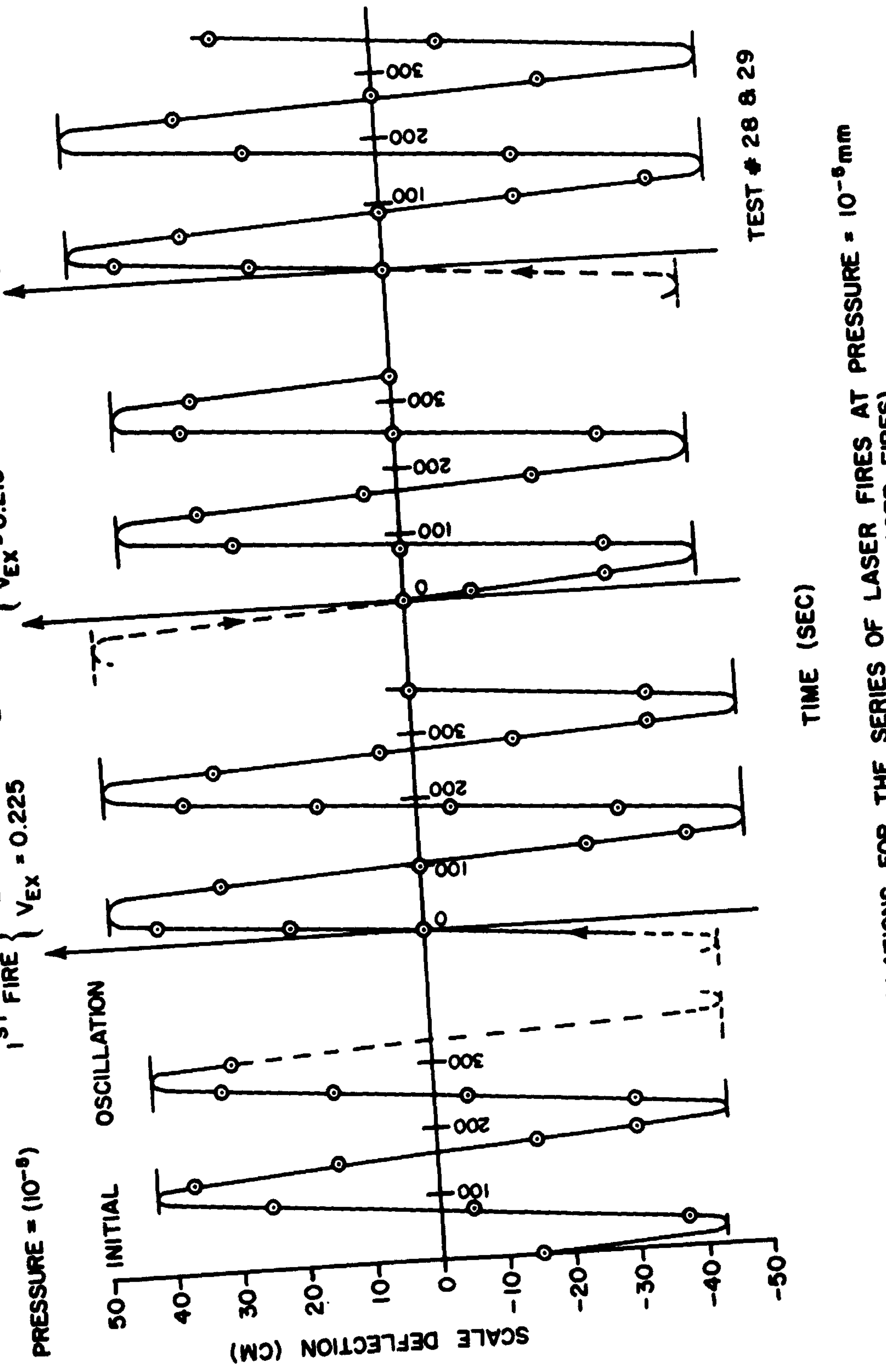

FIG.11A PLOTTED OSCILLATIONS FOR THE SERIES OF LASER FIRES AT PRESSURE = 10^{-6}mm OF Hg (INITIAL OSCILLATION AND FIRST THREE LASER FIRES)

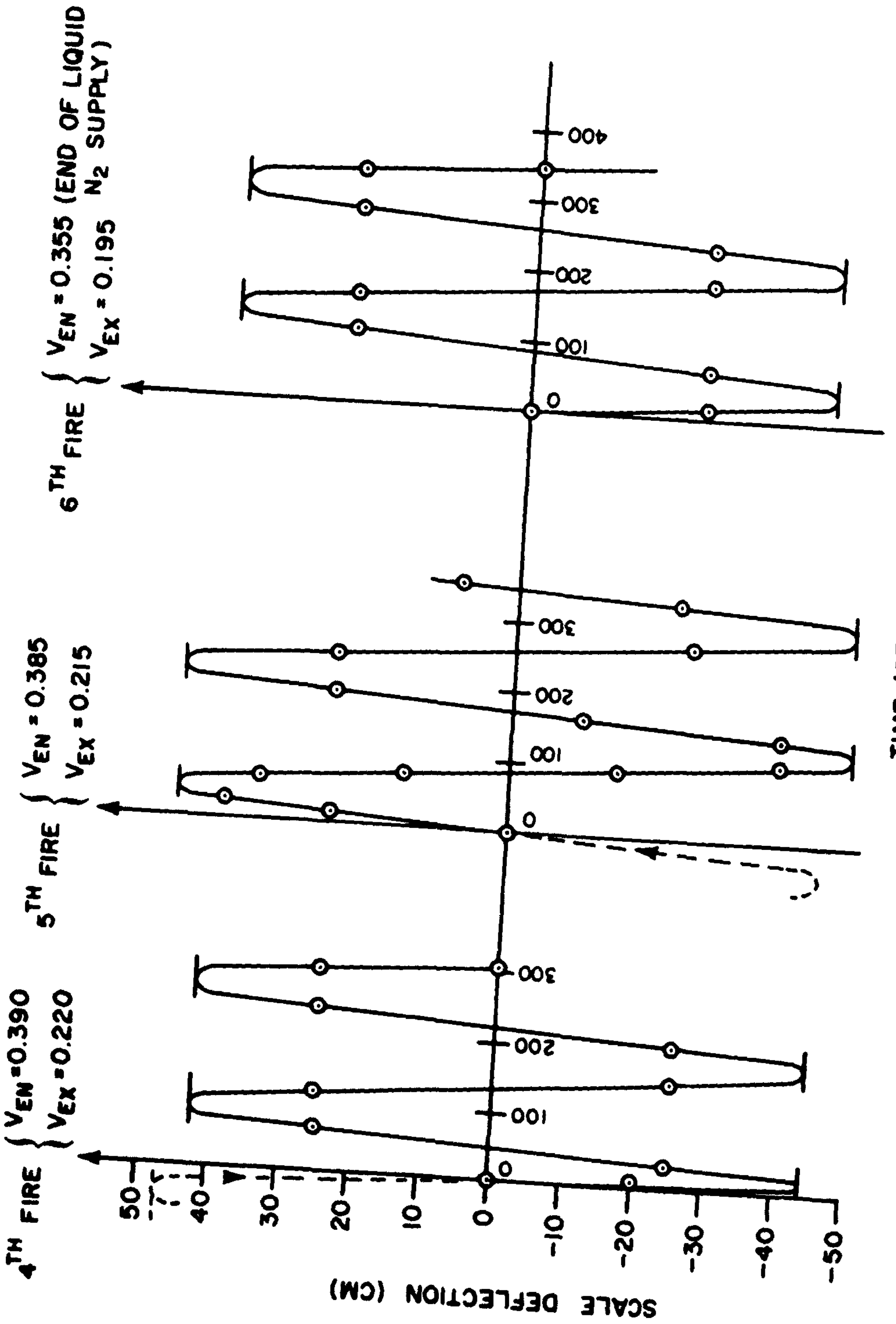

FIG. 11B REMAINING THREE LASER FIRES

TEST #29 (CONT)

suspension to its initial condition of oscillation. This result indicated that the deflection was due to an impulse such as photon momentum change on reflection from the instrument vanes. To determine the degree of repeatability of this observation, the laser was fired four more times for alternate directions of rotation of the suspension, and the data has been plotted on Figs. 11A and 11B for all six laser fires. The horizontal tangent lines in Figs. 11A and 11B are drawn for the peak readings which were observed. These peak values have been tabulated and are given consecutively in Table III. In this table, the first column gives the peak number as counted consecutively in time. The second column gives the initial oscillation and the number of the laser fire for which the peaks are being observed. The direction of rotation of the suspension at laser fire is given as positive or negative in the third column. The values of entrance and exit photocell voltages are given in the next two columns. The positive and negative peak deflections are given under the heading of "Peak deflection". The average values of the positive and negative peak deflections are given under "Max" and "Min" of the column "Average peak deflection". The averages of the positive and negative _change_ in peak readings are given in the last column, and represent the changes in deflection due

TABLE III. Observed peak deflections at P = 10^{-5}mm of Hg
(Large initial amplitudes)

Peak No.	Laser fire No.	Direction of rotation (+ or -)	V_{en} (volts)	V_{ex} (volts)	Peak deflection (cm)	Av peak deflection Max (cm)	Av peak deflection Min (cm)	Av change in peak deflection[a] (cm)
1	Initial Oscil- lation	----------------------			-42.6			
2					+42.5			
3					-43.5			
4					+42.4			
5					-43.5	+42.4	-43.2	---
6	1	(+)	0.400	0.225	+47.2			
7					-48.5			
8					+47.0			
9					-48.2	+47.1	-48.4	+5.0
10	2	(-)	0.390	0.215	-43.5			
11					+42.2			
12					-43.2			
13					+42.0	+42.1	-43.4	-5.0
14	3	(+)	0.380	0.220	+47.3			
15					-48.5			
16					+47.2			
17					-48.4	+47.2	-48.4	+5.0
18	4	(-)	0.390	0.220	-44.0			
19					+42.5			
20					-44.0			
21					+42.2	+42.4	-44.0	-4.6
22	5	(+)	0.385	0.215	+46.6			
23					-48.1			
24					+46.4			
25					-48.0	+46.5	-48.0	+4.0
26	6	(-)	0.355	0.195	-43.2			
27					+41.7			
28					-43.1			
29					+41.5	+41.6	-43.2	-4.8

[a] The average of the values in this column is 4.7 cm with an average deviation of ±0.3 cm.

to the laser fires. The average of the magnitudes of the values given in the last column of Table III (10^{-5} mm) is 4.7 cm.

The observations made at 10^{-5} mm of Hg for "small initial amplitudes" following the same procedure, are given in Table IV where the column headings are identical with those of Table III. The average change in deflection was found to be 5.5 cm, resulting in an average change at 10^{-5} mm, of 5.1 cm. The mean deviation of these results was ± 8%.

Results were obtained following the same procedure at the pressures of 4.5 x 10^{-5} and 8.2 x 10^{-5} mm of Hg. These results are given in Tables V and VI respectively. The average change in deflection at 4.5 x 10^{-5} mm of Hg. calculated from the results given in Table V was found to be 5.0 cm. At 8.2 x 10^{-5} mm, the average change was 4.4 cm.

3. Higher pressure results. A typical plot of the observed oscillations in the higher pressure region is shown in Fig. 12 taken at 5.2 x 10^{-4} mm of Hg. As described in Chap. II, the procedure in the higher pressure region was to first record the initial oscillation, as shown in Fig. 12, then to fire the laser once with the suspension rotating in the positive direction. It may be clearly seen from Fig. 12 that spurious gas effects control the instrument deflection.

TABLE IV. Observed peak deflections at $P = 10^{-5}$ mm of Hg
(Small initial amplitudes)

Peak No.	Laser fire No.	Direction of rotation (+ or -)	V_{en} (volts)	V_{ex} (volts)	Peak deflection (cm)	Av peak deflection Max (cm)	Av peak deflection Min (cm)	Av change in peak deflection[a] (cm)
1	Initial Oscil-lation	....			-9.0			
2					+10.0			
3					-8.9			
4					+10.0	+10.0	-9.0	----
5	1	(+)	0.400	0.220	+15.9			
6					-12.5			
7					+15.4			
8					-13.0	+15.6	-12.8	+4.7
9	2	(-)	0.400	0.220	-8.0			
10					+8.5			
11					-8.2			
12					+8.0	+8.2	-8.1	-6.0
13	3	(+)	0.405	0.230	+13.5			
14					-14.5			
15					+13.1			
16					-14.3	+13.3	-14.4	+5.7
17	4	(+)	0.400	0.215	+19.3			
18					-17.9			
19					+19.7			
20					-17.5	+19.5	-17.7	+4.8
21	5	(+)	0.400	0.225	+25.0			
22					-23.5			
23					+24.3			
24					-24.2	+24.6	-23.8	+5.5
25	6	(-)	0.410	0.235	-17.6			
26					+17.3			
27					-17.7			
28					+17.6	+17.4	-17.7	-6.6
29	7	(+)	0.410	0.223	+23.9			
30					-22.0			
31					+23.9			
32					-22.0	+23.9	-22.0	+5.4

[a] The average of the values in this column is 5.5 cm with an average deviation of ±0.5 cm.

TABLE V. Observed peak deflections at $P = 4.5 \times 10^{-5}$mm of Hg

Peak No.	Laser fire No.	Direction of rotation (+ or -)	V_{en} (volts)	V_{ex} (volts)	Peak deflection (cm)	Av peak deflection Max (cm)	Av peak deflection Min (cm)	Av change in peak deflection [a] (cm)
1	Initial	....			-4.0			
2	Oscil-				+2.3			
3	lation				-4.1	+2.3	-4.0	---
4	1	(+)	0.380	0.225	+6.7			
5					-9.6			
6					+6.8			
7					-9.6			
8					+7.0			
9					-9.4	+6.8	-9.6	+5.0
10	2	(-)	0.380	0.222	-3.7			
11					+2.0			
12					-3.5			
13					+2.0	+2.0	-3.6	-5.4
14	3	(+)	0.380	0.210	+6.1			
15					-8.3			
16					+6.1			
17					-8.4	+6.1	-8.4	+4.4
18	4	(-)	0.380	0.210	-4.1			
19					+1.5			
20					-4.0			
21					+1.5	+1.5	-4.0	-4.5
22	5	(+)	0.390	0.230	+6.8			
23					-9.0			
24					+7.2			
25					-9.0	+7.0	-9.0	+5.2
26	6	(-)	0.380	0.220	-4.5			
27					+1.9			
28					-4.5			
29					+1.8			
30					-4.2	+1.8	-4.4	-4.9
31	7	(+)	0.390	0.230	+7.3			
32					-9.7			
33					+7.4			
34					-9.6	+7.4	-9.6	+5.3

[a] The average of the values in this column is 5.0 cm with an average deviation of ±0.3 cm.

TABLE VI. Observed peak deflections at $P = 8.2 \times 10^{-5}$ mm of Hg

Peak No.	Laser fire No.	Direction of rotation (+ or -)	V_{en} (volts)	V_{ex} (volts)	Peak deflection (cm)	Av peak deflection Max (cm)	Av peak deflection Min (cm)	Av change in peak deflection[a] (cm)
1	Initial Oscil- lation	....			+7.0			
2					-5.4			
3					+7.0			
4					-5.3	+7.0	-5.4	---
5	1	(+)	0.370	0.220	+11.7			
6					-10.9			
7					+11.8			
8					-10.8	+11.8	-10.8	+5.1
9	2	(-)	0.360	0.200	-6.7			
10					+7.0			
11					-6.4			
12					+7.2	+7.1	-6.6	-4.4
13	3	(+)	0.365	0.200	+10.8			
14					-10.5			
15					+10.7			
16					-10.0			
17					+10.5			
18					-10.1			
19					+10.0	+10.7	-10.3	+3.6
20	4	(-)	0.370	0.210	-6.0			
21					+4.8			
22					-5.5			
23					+4.8			
24					-5.1			
25					+4.8			
26					-5.0			
27					+4.5			
28					-4.9	+4.7	-5.3	-5.4
29	5	(+)	0.385	0.215	+8.6			
30					-9.5			
31					+8.7			
32					-9.3	+8.6	-9.4	+4.0
33	6	(-)	0.390	0.210	-5.5			
34					+4.5			
35					-5.5			
36					+4.3	+4.4	-5.5	-4.0
37	7	(+)	0.390	0.215	+8.4			
38					-10.0			
39					+8.5			
40					-9.8	+8.4	-9.9	+4.2

[a] The average of the values in this column is 4.4 cm with an average deviation of ± 0.5 cm.

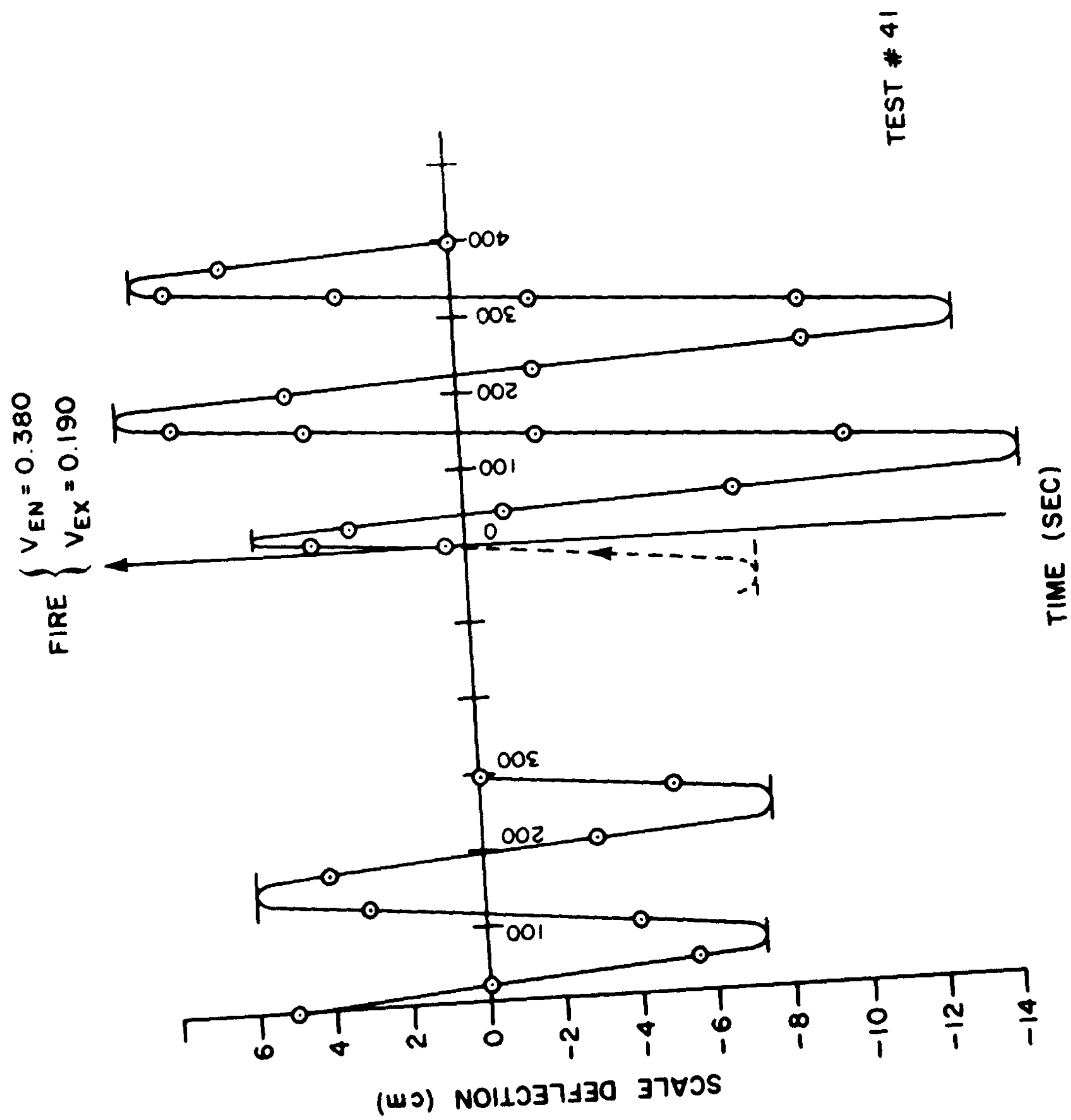

FIG.12 OSCILLATIONS OBTAINED AT PRESSURE = 5.2×10^{-4} mm OF Hg

Although the initial rotation is in the positive direction when the laser is fired, the first peak after fire is decreased in amplitude, and a negative peak larger than the initial value is produced. This indicates a long time heating effect with a force direction opposite to that expected for front surface heating of the vane. This effect has been observed by others, and is generally referred to as "spurious gas effects".[42] A deflection, for the purpose of this experiment, may be calculated from Fig. 12 on the basis of the second peak (negative) after laser fire. The difference between this peak and the initial negative peak has been defined as the change in deflection. Its sign is negative because of the reversing effect observed. At 3.4×10^{-4} mm the average change in deflection for three separate laser fires was found to be -6.0 cm. For three separate laser fires at 5.2×10^{-4} mm, the average change in deflection was found to be -9.0 cm.

4. Deflection versus pressure. The observed deflections over the pressure range investigated are shown in Fig. 13. The dependence of deflection change on pressure may be seen to disappear as the pressure is reduced from 5.2×10^{-4} to about 5×10^{-5} mm. Below this, down to 10^{-5} mm, the deflection change remains constant independent of pressure. The recorded

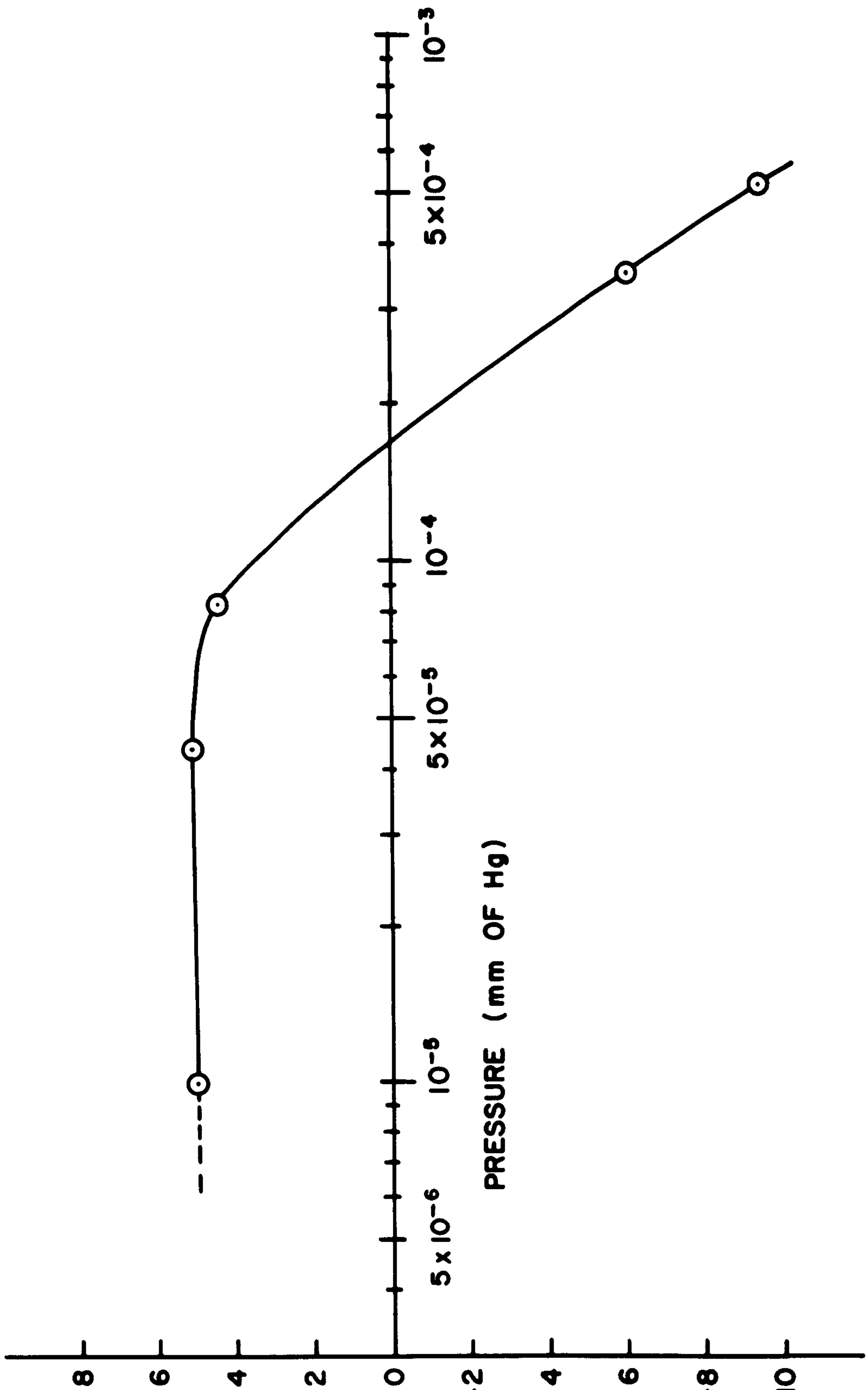

FIG.13 AVERAGE SCALE DEFLECTION VERSUS PRESSURE FOR SERIES OF LASER FIRES AT EACH PRESSURE

deflection at 10^{-5} mm, on Fig. 13, was calculated from both the large initial amplitude data given in Table III and the small initial amplitude data given in Table IV. The laser crystal temperature and capacitor bank voltage were held approximately the same for each laser actuation, as described in Chap. II, in order to maintain constant laser energy.

5. Deflection versus laser energy. Observations of deflection change as a function of relative laser energy, as measured by the entrance photocell (Fig. 3), are shown graphically in Fig. 14. The procedure is described in detail in Sec. 3, Chap. II, the main feature being that each point was determined from an average of the deflection changes due to a pair of laser fires. One laser fire is triggered for a positive initial rotation, and the second for a negative initial rotation with approximately the same output energy for each pair. It may be seen from the curve that below laser threshold[43], there is no instrument deflection. Since there is no laser energy, this is a reasonable result. There is, however, some photocell voltage apparently caused by the Xe flash tube. This may be explained by referring to the experimental setup of Fig. 3. Note that vane 1 of the instrument is further away from the laser than

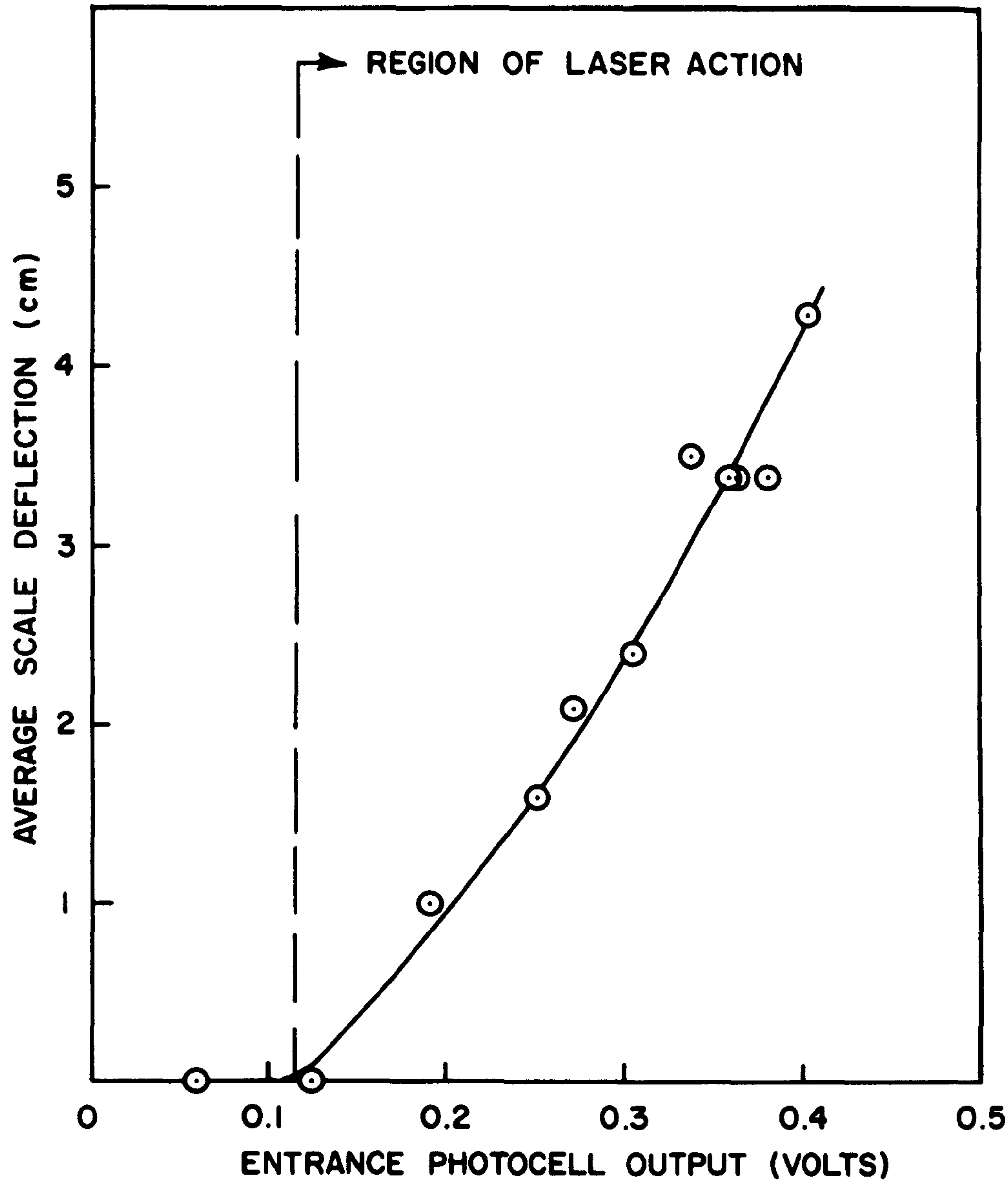

FIG. 14 AVERAGE OBSERVED SCALE DEFLECTION VERSUS RELATIVE INCIDENT ENERGY (PHOTOCELL OUTPUT) AT PRESSURE = 10^{-5} mm OF Hg

the entrance photocell.[44] Because of this additional distance, a fraction of the diverging Xe flash tube light may be reflected to the photocell with a negligible amount of energy reaching vane 1 of the instrument. This would result in some photocell current with negligible contribution to instrument deflection. To give some idea of the Xe energy, other than the laser wavelength at (6943A), that may affect the photocell, a plot has been made of the 925 photocell sensitivity superimposed on the No. 70 filter response curve of Fig. 6. This is shown in Fig. 15. The pass band at half power, as may be seen from Fig. 15, was approximately 6700 to 9600 A. The photocell voltage of 0.12 volts (Fig. 14) may be considered, therefore, to be in the nature of a bias which must be subtracted from all photocell readings. This was further verified by the fact that below laser threshold, although there were readings of entrance photocell voltage, there were no exit photocell readings. A corrected curve of deflection versus photocell voltage is shown by the solid curve in Fig. 16. The dashed curve is a replot of the observed results of Fig. 14.

6. Photocell calibration and comparison. The relation between incident laser energy on the vacuum chamber window and photocell voltage may now be obtained by applying Fig. 10, the instrument sensitivity curve drawn from Eq. (31), to the

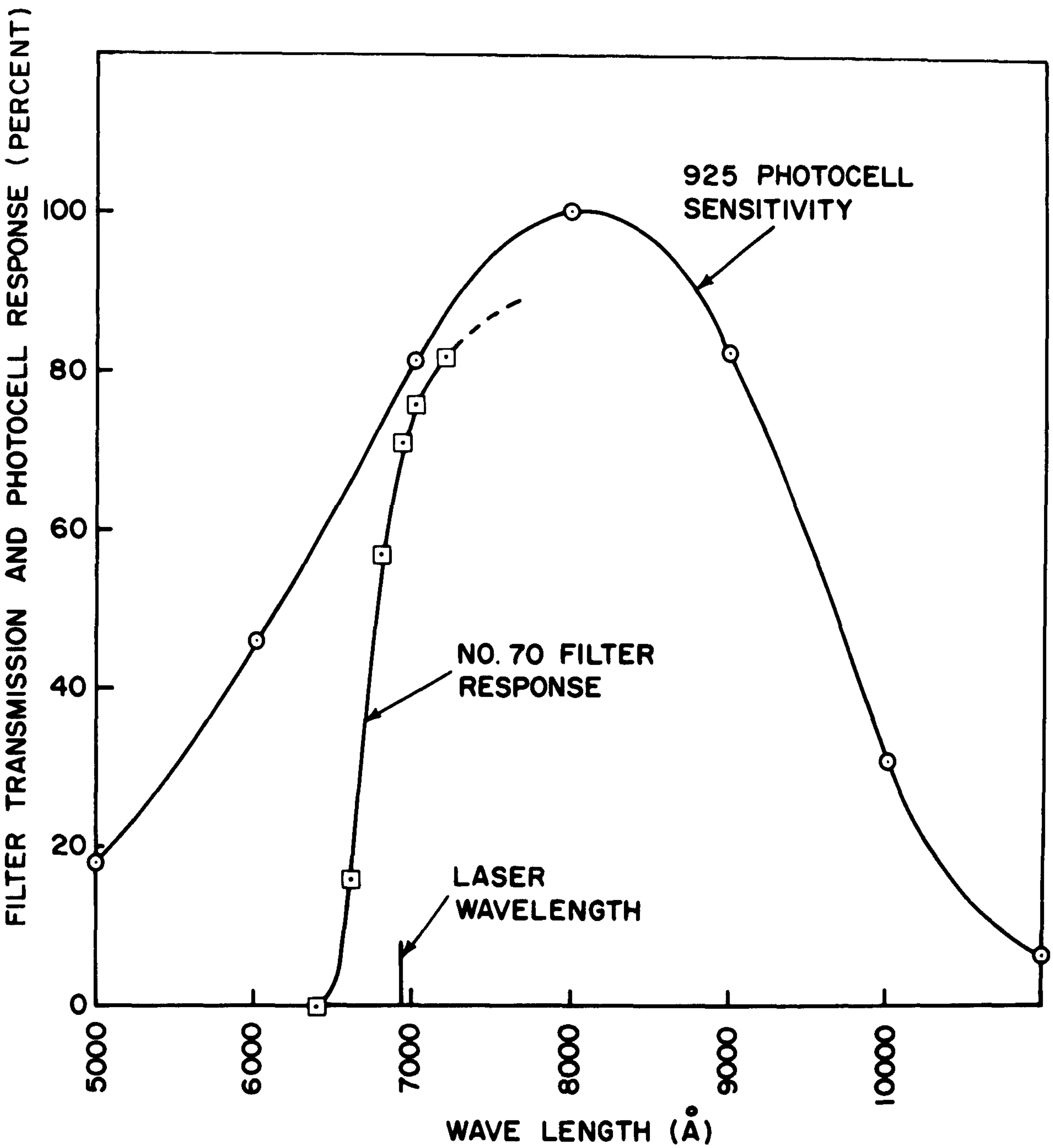

FIG.15 SUPERPOSITION OF NUMBER 70 FILTER RESPONSE AND 925 PHOTOCELL SENSITIVITY

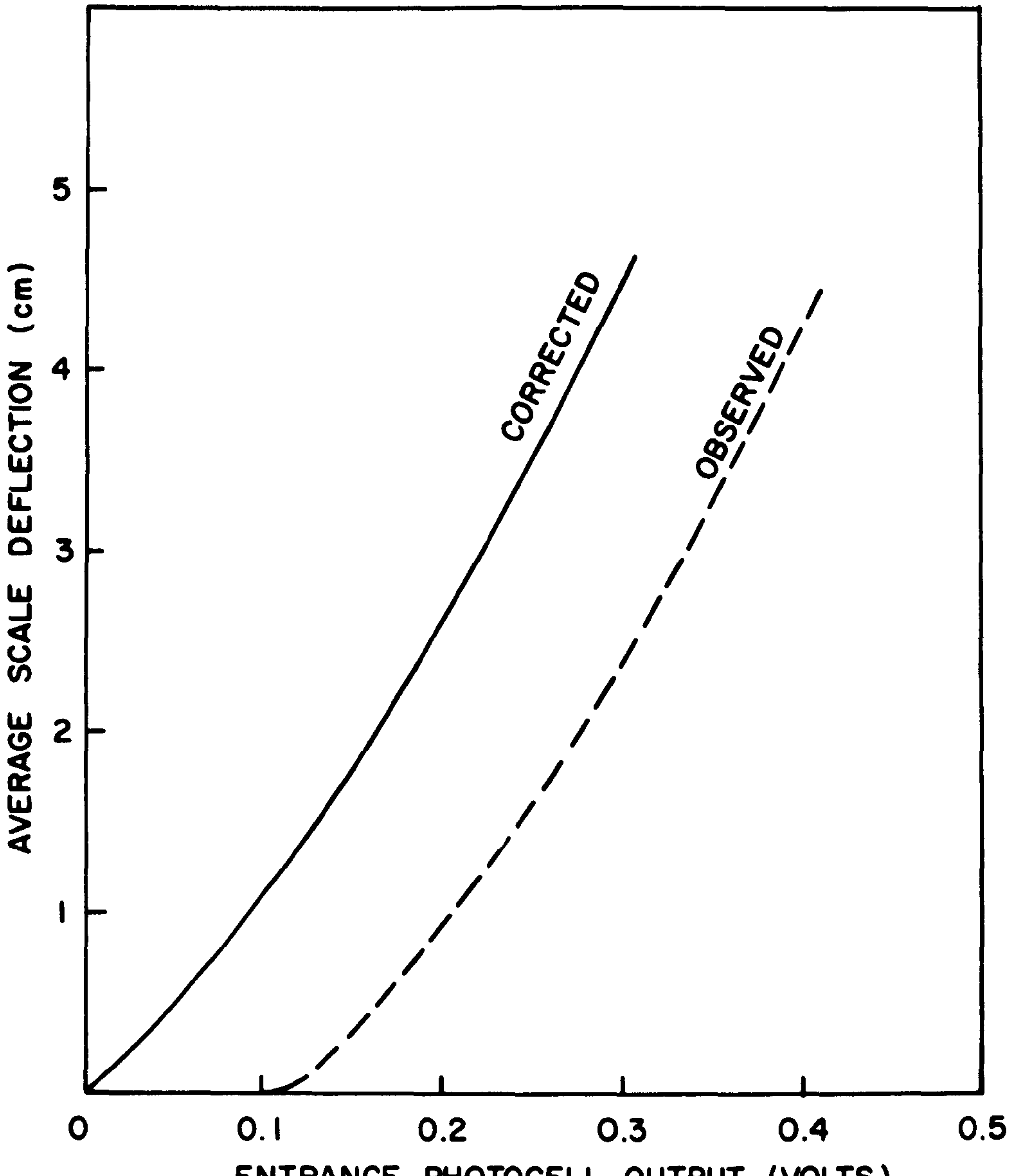

FIG. 16 CORRECTED CURVE OF SCALE DEFLECTION VERSUS ENTRANCE PHOTOCELL OUTPUT

corrected curve of deflection vs photocell voltage, of Fig. 16. The result is shown in Fig. 17 by the solid curve which represents the photocell calibration by the momentum transfer experiment. The dashed curve, shown in Fig. 17, represents the photocell calibration using the calorimeter. The same photocell correction described in Sec. 5 of this chapter has been applied to the observed photocell curve of Fig. 8, since the blackbody was placed in the same relative position as vane 1. In an attempt to correct the energy collected by the lens window of the calorimeter, a feature not present in the vacuum chamber window, a further correction has been applied to the calorimeter curve. When the photocell bias voltage was subtracted, the calorimeter curve was shifted to start from the origin of the coordinate axes. This corresponded to subtracting the small collected energy associated with the photocell bias.

It will be observed that there is reasonable agreement between the two methods below about one joule. Above this, the calorimeter curve deviates appreciably from linearity. As a result it indicates higher laser energies, for the same photocell outputs, than the momentum transfer instrument. This may be due to reduction in mass of the blackbody material due to vaporization.[45] Higher temperatures would

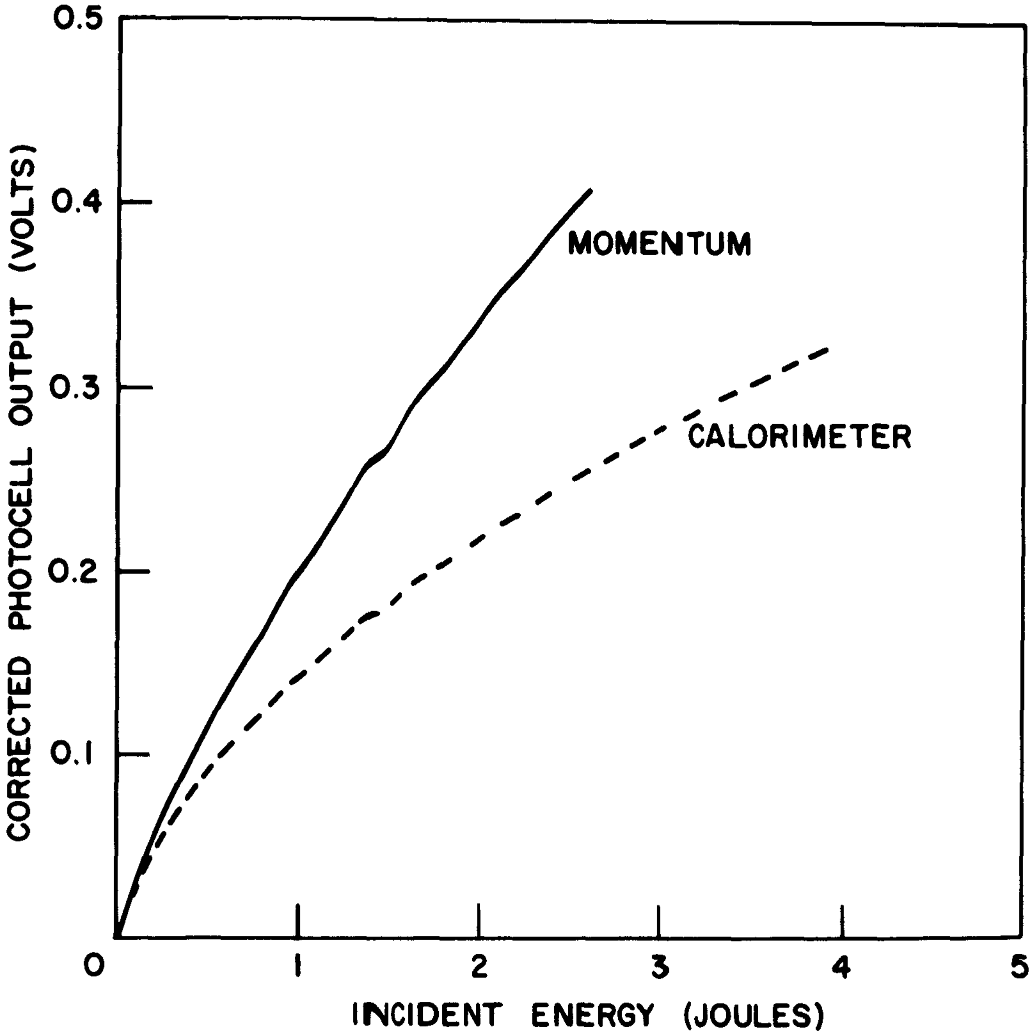

FIG. 17 COMPARISON OF PHOTOCELL CALIBRATION CURVES BY MOMENTUM MEASUREMENT AND BY CALORIMETER

therefore result, giving higher thermocouple outputs and higher apparent energies.

According to the data there is a slight nonlinearity between the photocell output and the deflection as indicated in Fig. 14 and again in the momentum curve of Fig. 17. It is reasonable to assume that this nonlinearity is in the photocell, possibly due to the shadow of the anode on the cathode.

From the momentum curve of Fig. 17 it can be seen that for an entrance photocell voltage of 0.4 volts, the laser energy incident on the vacuum chamber window was approximately 2.5 joules. To determine the laser energy which results in this photocell voltage, the attenuation of the optical system ahead of the momentum transfer instrument must be accounted for (see Fig. 3). This attenuation, K, may be found from the values given in Table I.

$$K = (0.71)(0.80)(0.865) = 0.49 \tag{44}$$

The laser output, E, at $V_{EN} = 0.4$ volts is, therefore,

$$E = 2.5/0.49 = 5.1 \text{ joules} \tag{45}$$

This was approximately the energy at which the laser was maintained in obtaining the data on deflection vs pressure in this experiment.

CHAPTER V

SUMMARY AND CONCLUSIONS

The results obtained in this work confirm that useful measurements of the energy in a laser beam may be obtained by reflecting the beam from its original path in order to transfer the photon momentum to a calibrated mechanical system operating on the principle of a torsional ballistic pendulum. The use of a pair of reflectors provided several advantages. The incident laser beam could be brought out of the instrument after the double reflection and used for a simultaneous experiment. In addition, the need for pinning down the suspension was eliminated by the fact that there was very little unbalanced force, or that nearly a pure couple resulted which gave higher instrument sensitivity. For high energy laser beam measurements, the instrument offers advantages over the use of calorimeters since it does not require long stabilization times, nor does it absorb the energy, with good reflectors.

This has been demonstrated by the design, construction, and operation of a reflecting vane measuring instrument having a torsional ballistic element. The deflection of this element was found to be proportional to laser energy after applying a photocell bias correction.

The instrument was designed and constructed on the basis of calculations of the momentum transfer which were verified experimentally. The change in peak deflection due to a laser pulse was found to be independent of any rotational motion present before laser actuation. This introduced a measurement simplification whereby damping out of the oscillations between measurements was unnecessary.

The proper operating pressure in which to perform the momentum experiment was found by reducing the pressure until gas effects disappeared. An interesting gas effect was observed which appears worthy of future research because of its systematic behavior. In the region where gas effects became negligible, it was verified that deflections were due to the photon momentum of the laser beam.

For this instrument the calculated sensitivity was 2.55 cm/joule. Observed results indicated that this instrument gave a more accurate measure of the energy than the commercial calorimeter with which it was compared. It is estimated that the measurements could be made to an accuracy of ± 0.04 joule. A detailed study of calorimetry problems is suggested by the difference in the two methods. This could well be another problem for future research.

APPENDIX A

MOMENT OF INERTIA CALCULATIONS

Mass of each reflection vane	0.267 gm
Mass of wax joints	0.015 gm
Distance between centers of vanes[a]	7.40 cm

Letting I_1 = The moment of inertia of vanes and joints
and M_1 = The mass of vanes and joints

$$I_1 = M_1R^2 = \left[(2)(0.267) + (0.015)\right](7.40/2)^2$$

$$I_1 = 7.50 \text{ gm cm}^2$$

Mass/unit length of cross arm material (Al)[b]	$4.48\text{x}10^{-3}$ gm/cm
Length of cross arm.	7.40 cm

Letting I_2 = The moment of inertia of cross arm,
and M_2 = The mass of cross arm

$$I_2 = M_2L^2/12 = (7.40)(4.48\text{x}10^{-3})(7.40)^2/12$$

$$I_2 = 0.15 \text{ gm cm}^2$$

Diameter of scale mirror	2.50 cm
Mass of scale mirror	0.267 gm

Letting I_3 = The moment of inertia of scale mirror,
and M_3 = The mass of the mirror

$$I_3 = M_3r^2/4 = (0.267)(2.50)^2/16$$

$$I_3 = 0.10 \text{ gm cm}^2$$

Letting I = Total moment of inertia of suspension,[c]

$$I = I_1 + I_2 + I_3 = 7.50 + 0.15 + 0.10$$

$$I = 7.75 \text{ gm cm}^2$$

[a] See Figs. 1 and 2.
[b] See Sec. 1, Chap. II.
[c] The contribution of the vertical portion of the Al structure has been assumed negligible.

APPENDIX B

CALCULATIONS FROM CHAPTER III

Instrument sensitivity[a]

$$d_s - d_o = 2(1 + \Gamma_v^2)T_w RDU/c(kI)^{\frac{1}{2}} \quad (30)$$

$$= 2\left[1+(0.75)^2\right](0.92)(7.40/2)(200)(10^7)/(3x10^{10})(7.75x10^{-2})^{\frac{1}{2}}$$

$$= (1.56)(0.92)(7.40)(200)(10^{-2})/(3)(7.75)^{\frac{1}{2}}$$

$$d_s - d_o = 2.55 \text{ cm/joule} \quad (31)$$

Translational motion

$$V_y = T_w U(1 - \Gamma_v^2)/Mc \quad (21)$$

$$V_y = (0.92)(10^7)(1 - 0.56)/(0.98)(3 \times 10^{10})$$

$$V_y = (0.92)(0.44)(10^{-3})/(0.98)(3)$$

$$V_y = 1.37 \times 10^{-4} \text{ cm/sec.} \quad (32)$$

[a]See Table II, page 34.

NOTES

[1] T. H. Maiman, Nature, 187, 493, (1960).

[2] Raytheon Instrument Corporation.

[3] Trion Instrument Corporation (later changed to Laser Systems Center/Lear Siegler Corporation). The laser used in this experiment was purchased from this company.

[4] The commercial calorimeter used in this experiment had to be replaced, for this reason, by the company from which it was purchased.

[5] Large Government and private industry expenditures have been made for research of this nature.

[6] J. C. Maxwell, Elec. and Mag. Vol. 2, 1st ed. (Oxford University Press, New York, 1873).

[7] S. Bartoli, Sopra i movimenti prodotti della luce e dal calore, (Florence, Le Monnier, 1876).

[8] P. Lebedew, Ann. Physik, 11, 433, (1901).

[9] E. F. Nichols and G. F. Hull, Phys. Rev., 5, 307, (1901).

[10] J. D. Tear, J. Opt. Soc. Am. & Rev. Sci. Instr., 11, 135, (1925).

[11] Tear used a silver vane torsion balance and attempted to operate in a high pressure region.

[12] This was done by plotting high pressure "radiometer deflections" vs "radiation pressure deflections" and assigning "zero pressure" to zero radiometer deflection.

[13] See reference 10, p. 136.

[14] The calorimeter used in this experiment was purchased from the Trion Instrument Corporation (see reference 3).

[15] The vacuum deposition was performed in the Naval Ordnance Laboratory (NOL) Glass Laboratory, which is under the supervision of Mr. W. L. Clark.

[16] H. V. Neher, Am. J. Phys., 29, 666, (1961).

[17] Professor Karl F. Herzfeld made the suggestion to me, for a nonmagnetic mirror, to induce eddy currents in the aluminum for damping. Such an eddy current effect must also be present in the control of oscillation by the method used in this experiment.

[18] The wire was manufactured by the Sigmund Cohn Corporation, from whom this value was obtained.

[19] See reference 3.

[20] See reference 14.

[21] This information was obtained through private communications with the Operations Manager of the Laser Systems Center (see reference 3).

[22] These values and the calculations are given in Appendix A.

[23] See reference 10, p. 136.

[24] Defined in Chap. IV, Results and Discussion.

[25] See reference 24.

[26] The positive direction of rotation has been defined in this paper as the direction of rotation for which vane 1 (Figs. 3 and 9) moves away from the laser. It has also been defined on p. 17 with reference to Fig. 2.

[27] This condition could be obtained with the laser crystal at room temperature.

[28] This was done with the cooperation of Mr. P. R. Wessel of NOL who made available his reflectivity apparatus for these measurements.

29 The Phillips gage was connected to a vacuum system whose pressure readings were obtained from an ionization gage which had been calibrated in that system by a McLeod gage.

30 This approximation is correct, in this experiment, to better than 1.7%, this maximum error occurring at a scale deflection of 48 cm.

31 See Appendix A.

32 See reference 18.

33 See Sec. I, Chap. II, and Sec. 7, Chap. III.

34 See Fig. 2.

35 See reference 34.

36 This value was measured at the same angle of incidence as in the experiment, 45°.

37 These measurements are given in Appendix A.

38 H. S. Taylor and S. Glasstone, Treatise on Physical Chemistry Vol. 2 (D. Van Nostrand Company, Inc., New York, 1952).

39 This is for the simple case given by K. F. Herzfeld and H. M. Smallwood in Eq. (11.2), p. 42, of the Kinetic Theory of Gases Chapter of reference 38.

40 It was not desirable to bake, or similarly heat treat the instrument, for obtaining ultra-high vacuums.

41 J. J. Cook, W. L. Flowers, and C. B. Arnold, Proc. Inst. Radio Engrs., 1693, (July, 1962).

42 See p. 136 of reference 10.

43 This condition was with full pump energy. See reference 27.

44 This additional distance was approximately 20 cm.

45 See Chap. I, and reference 4.

SELECTED BIBLIOGRAPHY

1. Books

Bartoli, S., Sopra i movimenti prodotti della luce a dal calore, (Florence, Le Monnier, 1876).

Jenkins, F. A., and White, H. E., Fundamentals of Optics, (McGraw-Hill Book Co., Inc. New York, N. Y., 1957) 3rd ed.

Maxwell, J. C. Electricity and Magnetism, (Dover Publications, Inc., New York, N. Y., 1954) 3rd ed.

Slater, J. C., and Frank, N. H., Electromagnetism. (McGraw-Hill, Book Co., Inc., New York, N. Y. 1947).

Strong, J., Procedures in Experimental Physics. (Prentice-Hall, Inc., Englewood Cliffs, N. J., 1946).

Taylor, H. S., and Glasstone, S., Treatise on Physical Chemistry, Chap. 1 (D. Van Nostrand Co., Inc., Princeton, N. J. 1951) Vol. 2, 3rd ed.

2. Periodicals

Einstein, A., Z. Physik, 27, 1, 1924. The Radiometer.

Cook, J. J., Flowers, W. L., and Arnold, C. B., Proc. Inst. Radio Engrs., 1693, (July 1962), Letter: Measurement of Laser Output by Light Pressure.

Hettner, G., Z. Physik, 27, 12, 1924: The Radiometer.

Lebedew, P., Ann. Physik, 11, 433, (1901): Pressure of Light.

Maiman, T. H., Nature, 187, 493, (1960): Stimulated Optical Radiation in Ruby Masers and Superconductors.

March, H. E., Condon, E., and Loeb, L. B., J. Opt. Soc. Am. & Rev. Sci. Instr. 11, 257, (1925): The Theory of the Radiometer.

Neher, H. V., Am. J. Phys., 29, 666, (1961): Light-Pressure Tube.

Nichols, E. F. and Hull, G. F., Phys. Rev., 13, 307 (1901): A Preliminary Communication on the Pressure of Heat and Light Radiation.

Pettit, E., J. Opt., Soc. Am., 10, 267, (1925): The Use of the D'Arsonval Galvanometer in Radiation Measurements.

Tear, J. D., J. Opt. Soc. Am., 10, 81, (1924): The Nichols Radiometer.

Tear, J. D., J. Opt. Soc. Am. & Rev. Sci. Instr., 11, 135, (1925): A Torsion Balance for Measuring Radiation Pressure.

3. Miscellaneous

Eastman Kodak Corp., Kodak Wratten Filters for Scientific and Technical Use (Rochester, N. Y.).

Edgerton, Germeshausen & Grier, Inc., Xenon Flash Tubes, Trigger Transformers, Chokes, Bulletin 1001 (Boston, Mass).

General Electric Corp., General Electric Flash Tube Data Manual (Cleveland, Ohio).

Laser Systems Center, Calorimeter Data Sheet (Private Communication, Ann Arbor, Mich.).

Laser Systems Center, LS-4 Laser System (Instruction Manual, Ann Arbor, Mich.).

Radio Corporation of America, Tube Handbook HB-3, vol. 9-10 Harrison, N. J.).

Sanborn Co., Dual Channel DC Amplifier-Recorder, Model 322, Instruction Manual.

Zacharias, J. R., P.S.S.C. Film, Pressure of Light, (Modern Learning Aids, New York, N. Y. 1959).

DISTRIBUTION

	Copies
Chief, Bureau of Naval Weapons Attn: Library, DIS 3 Washington 25, D. C.	4
Bureau of Naval Weapons (RMMO-22) Washington 25, D. C.	1
Bureau of Naval Weapons (RREN-4) Washington 25, D. C.	1
Bureau of Naval Weapons (RUDC-4B) Washington 25, D. C.	1
Defense Documentation Center Cameron Station Alexandria, Va.	10
Office of Naval Research Washington 25, D. C. Code 104	2

CATALOGING INFORMATION FOR LIBRARY USE

BIBLIOGRAPHIC INFORMATION

	DESCRIPTORS	CODES		DESCRIPTORS	CODES
SOURCE	NOL technical report	NOLTR	SECURITY CLASSIFICATION AND CODE COUNT	Unclassified-22	U022
REPORT NUMBER	63-82	630082	CIRCULATION LIMITATION		
REPORT DATE	10 September 1963	0963	CIRCULATION LIMITATION OR BIBLIOGRAPHIC		
			BIBLIOGRAPHIC (SUPPL., VOL., ETC.)		

SUBJECT ANALYSIS OF REPORT

DESCRIPTORS	CODES	DESCRIPTORS	CODES	DESCRIPTORS	CODES
Measurement	MEAU	Simultaneous	SIMT		
Energy	ENER	Equipment	EQUI		
Laser	LASE	Theory	THEY		
Beam	BEAM	Experiment	EXPE		
Pulsed	PULS	Reflection	REFL		
Transfer	TRAE	Reflector	REFE		
Photon	PHTO	Comparison	CMRI		
Momentum	MOTI	Calorimeters	CALM		
Ballistic	BALS	Pressure	PRES		
Torsional	TORS	Sensitivity	SENV		
Pendulum	PENU				
Instrument	INSM				

PRNC-NOL-5070/28 (5-62)

Naval Ordnance Laboratory, White Oak, Md.
(NOL technical report 63-82)
DETERMINATION OF THE ENERGY OF A PULSED BEAM BY TRANSFER OF THE PHOTON MOMENTUM TO A BALLISTIC TORSIONAL PENDULUM (U), by M. Stimler. 10 Sept. 1963. 70p. charts. BuWep task RREN-04-322/212/1/F008-21/02.

UNCLASSIFIED

This report presents the results of an experiment in which the photon momentum of a pulsed laser beam was used to make a fundamental measurement of the beam energy.

Abstract card is unclassified

1. Lasers - Energy
2. Pendulums, Ballistic
3. Pendulums, Torsion
I. Title
II. Stimler, Martin
III. Project

Naval Ordnance Laboratory, White Oak, Md.
(NOL technical report 63-82)
DETERMINATION OF THE ENERGY OF A PULSED BEAM BY TRANSFER OF THE PHOTON MOMENTUM TO A BALLISTIC TORSIONAL PENDULUM (U), by M. Stimler. 10 Sept. 1963. 70p. charts. BuWep task RREN-04-322/212/1/F008-21/02.

UNCLASSIFIED

This report presents the results of an experiment in which the photon momentum of a pulsed laser beam was used to make a fundamental measurement of the beam energy.

Abstract card is unclassified

1. Lasers - Energy
2. Pendulums, Ballistic
3. Pendulums, Torsion
I. Title
II. Stimler, Martin
III. Project

Naval Ordnance Laboratory, White Oak, Md.
(NOL technical report 63-82)
DETERMINATION OF THE ENERGY OF A PULSED BEAM BY TRANSFER OF THE PHOTON MOMENTUM TO A BALLISTIC TORSIONAL PENDULUM (U), by M. Stimler. 10 Sept. 1963. 70p. charts. BuWep task RREN-04-322/212/1/F008-21/02.

UNCLASSIFIED

This report presents the results of an experiment in which the photon momentum of a pulsed laser beam was used to make a fundamental measurement of the beam energy.

Abstract card is unclassified

1. Lasers - Energy
2. Pendulums, Ballistic
3. Pendulums, Torsion
I. Title
II. Stimler, Martin
III. Project

Naval Ordnance Laboratory, White Oak, Md.
(NOL technical report 63-82)
DETERMINATION OF THE ENERGY OF A PULSED BEAM BY TRANSFER OF THE PHOTON MOMENTUM TO A BALLISTIC TORSIONAL PENDULUM (U), by M. Stimler. 10 Sept. 1963. 70p. charts. BuWep task RREN-04-322/212/1/F008-21/02.

UNCLASSIFIED

This report presents the results of an experiment in which the photon momentum of a pulsed laser beam was used to make a fundamental measurement of the beam energy.

Abstract card is unclassified

1. Lasers - Energy
2. Pendulums, Ballistic
3. Pendulums, Torsion
I. Title
II. Stimler, Martin
III. Project

Naval Ordnance Laboratory, White Oak, Md.
(NOL technical report 63-82)
DETERMINATION OF THE ENERGY OF A PULSED BEAM BY TRANSFER OF THE PHOTON MOMENTUM TO A BALLISTIC TORSIONAL PENDULUM (U), by M. Stimler. 10 Sept. 1963. 70p. charts. BuWep task RREN-04-322/212/1/F008-21/02.

UNCLASSIFIED

This report presents the results of an experiment in which the photon momentum of a pulsed laser beam was used to make a fundamental measurement of the beam energy.

Abstract card is unclassified

1. Lasers - Energy
2. Pendulums, Ballistic
3. Pendulums, Torsion
I. Title
II. Stimler, Martin
III. Project

Naval Ordnance Laboratory, White Oak, Md.
(NOL technical report 63-82)
DETERMINATION OF THE ENERGY OF A PULSED BEAM BY TRANSFER OF THE PHOTON MOMENTUM TO A BALLISTIC TORSIONAL PENDULUM (U), by M. Stimler. 10 Sept. 1963. 70p. charts. BuWep task RREN-04-322/212/1/F008-21/02.

UNCLASSIFIED

This report presents the results of an experiment in which the photon momentum of a pulsed laser beam was used to make a fundamental measurement of the beam energy.

Abstract card is unclassified

1. Lasers - Energy
2. Pendulums, Ballistic
3. Pendulums, Torsion
I. Title
II. Stimler, Martin
III. Project

Naval Ordnance Laboratory, White Oak, Md.
(NOL technical report 63-82)
DETERMINATION OF THE ENERGY OF A PULSED BEAM BY TRANSFER OF THE PHOTON MOMENTUM TO A BALLISTIC TORSIONAL PENDULUM (U), by M. Stimler. 10 Sept. 1963. 70p. charts. BuWep task RREN-04-322/212/1/F008-21/02.

UNCLASSIFIED

This report presents the results of an experiment in which the photon momentum of a pulsed laser beam was used to make a fundamental measurement of the beam energy.

Abstract card is unclassified

1. Lasers - Energy
2. Pendulums, Ballistic
3. Pendulums, Torsion
I. Title
II. Stimler, Martin
III. Project

Naval Ordnance Laboratory, White Oak, Md.
(NOL technical report 63-82)
DETERMINATION OF THE ENERGY OF A PULSED BEAM BY TRANSFER OF THE PHOTON MOMENTUM TO A BALLISTIC TORSIONAL PENDULUM (U), by M. Stimler. 10 Sept. 1963. 70p. charts. BuWep task RREN-04-322/212/1/F008-21/02.

UNCLASSIFIED

This report presents the results of an experiment in which the photon momentum of a pulsed laser beam was used to make a fundamental measurement of the beam energy.

Abstract card is unclassified

1. Lasers - Energy
2. Pendulums, Ballistic
3. Pendulums, Torsion
I. Title
II. Stimler, Martin
III. Project